IN THE LYCOPHYTE *SELAGINELLA MARTENSII* IS THE "EXTRA-QT" RELATED TO ENERGY SPILLOVER? INSIGHTS INTO PHOTOPROTECTION IN ANCESTRAL VASCULAR PLANTS

LORENZO FERRONI[A], SALVATORE CUCUZZA[A], MARTINA ANGELERI[B], EVA-MARI ARO[B], CRISTINA PAGLIANO[C], MARTINA GIOVANARDI[A], COSTANZA BALDISSEROTTO[A], SIMONETTA PANCALDI[A]

[A] DEPT. OF LIFE SCIENCES AND BIOTECHNOLOGY, UNIVERSITY OF FERRARA, C.SO ERCOLE I D'ESTE 32 – 44121 FERRARA, ITALY

[b] Molecular Plant Biology, Dept. of Biochemistry, University of Turku, 20014 Turku, Finland

[c] Applied Science and Technology Department - BioSolar Lab, Politecnico di Torino, Viale T. Michel 5, 15121 Alessandria, Italy

Corresponding Author: Lorenzo Ferroni, lorenzo.ferroni@unife.it

ABSTRACT

Lycophytes are early diverging vascular plants, representing a minor group as compared to the dominating euphyllophytes, mostly angiosperms. Having maximally developed in a CO_2-rich atmosphere, extant lycophytes are characterized by a low carbon fixing capacity, which is compensated by a marked ability to induce the non-photochemical quenching of chlorophyll fluorescence (*NPQ*). Different kinetic components contribute to *NPQ*, in particular the fast relaxing high-energy quenching qE, the middle relaxing qT, and the slowly relaxing qI. Unlike angiosperms, lycophytes enhance the qT component under high light, originating from an "extra-qT". In this research, we analyze whether in *Selaginella martensii* the extra-qT can reflect a photosystem (PS) I-based quenching mechanism activated upon saturation of qE capacity. From comparative analyses of fluorescence quenching parameters, carbon fixation, in vivo low- and room-temperature fluorescence spectroscopy, and thylakoid protein phosphorylation, it is proposed that the extra-qT is not mechanistically separate from the ordinary qT. The results suggest a relationship between qT and photoprotective energy spillover to PSI, which is activated upon sensing the excitation energy pressure inside PSII and is possibly facilitated by phosphorylation of Lhcb6, a minor antenna protein of PSII. Energy spillover emphasizes 77 K fluorescence emission from PSI core (F714) and becomes more relevant at irradiance levels corresponding to the CO_2-limited, potentially photoinhibiting phase of photosynthesis. At the highest irradiances, when Lhcb6 phosphorylation potential has been saturated, the major LHCII increases in turn its phosphorylation level, probably leading to the full exploitation of PSI as a safe excitation sink. It is suggested that the low photosynthetic capacity of lycophytes could allow an easier experimental access to the use of PSI as a safe excitation quencher for PSII, a debated, emerging issue about thylakoid photoprotection in angiosperms.

KEYWORDS

Antenna phosphorylation, energy spillover, lycophytes, chlorophyll fluorescence, photoprotection, *Selaginella martensii*

HIGHLIGHTS

- Amplitude of the middle phase of *NPQ* relaxation, qT, correlates with the excitation energy pressure inside PSII
- Upon saturation of carbon fixing capacity, an extra-qT is enhanced in parallel with the relative fluorescence emitted by PSI core
- qT strongly correlates with the phosphorylation level of Lhcb6 antenna, but not of LHCII
- In lycophytes, a relationship between qT and photoprotective energy spill over to PSI is proposed

1. Introduction

During their very early evolution, vascular plants divided into the two well-differentiated lineages of lycophytes and euphyllophytes. Lycophytes formed the dominant vegetation up to the mid-Carboniferous period; their subsequent decline is considered as a “side effect” of their own intense photosynthetic activity, which progressively reduced the CO_2 availability in the atmosphere. Euphyllophytes - and, among them, angiosperms -, proved to be more competitive than lycophytes under a low CO_2 condition and soon replaced lycophytes in plant consortia, until the latter were reduced to only some 1250 extant species.

In the chloroplasts of lycophytes, the photosynthetic membrane components are essentially the same as in euphyllophytes and, more in general, in Viridiplantae. In Photosystem II (PSII), the absorbed energy is used to recover electrons from water to reduce an intersystem electron transport chain formed by plastoquinone, Cytochrome b_6f complex and plastocyanine. Photosystem I (PSI) oxidizes the chain, using light to move electrons up to the stromal $NADP^+$ acceptors through a ferredoxin-$NADP^+$ reductase (FNR). Operation of such intersystem electron transport is accompanied by the creation of the trans-thylakoid ΔpH exploited by the ATPsynthase to produce ATP. Both PSII and PSI are sensitive to excess light, the former being easily inactivated by an excess of excitons, the latter being more prone to the damage caused by excess electrons coming from PSII (Sonoike, 2011; Suorsa et al., 2012). A set of light-harvesting complexes serves the photosystems (LHCII and LHCI) and especially LHCII plays a key role in the regulation of the amount of excitons to be channeled to photosystems (Wientjes et al., 2013a; Grieco et al., 2015; Benson et al., 2015). Within the LHCII antenna protein family, Lhcb3 and Lhcb6 are found exclusively in land plants – lycophytes included - and are considered of great importance to PSII organization upon land conquest (Koziol et al., 2007). However, this concept has recently been challenged by the discovery of gymnosperms lacking such antennae (Kouřil et al., 2016).

Lycophytes apparently differ from euphyllophytes with regard to their photosynthetic efficiency, which seems to have remained unchanged since set at the CO_2-rich air condition characterizing the Devonian period. Because of their low carbon fixation, lycophytes experience a marked decline in the

maximum quantum yield of PSII upon increasing irradiance, and this is compensated by a noticeable ability to induce the non-photochemical quenching of chlorophyll fluorescence (*NPQ*; Ferroni et al., 2014).

NPQ is a useful technical parameter that quantifies any decrease in maximum PSII fluorescence F_M. For 30 years it has been usual to describe *NPQ* in kinetic terms, as a composite of processes relaxing in darkness in less than one minute, or in some 10 minutes, or taking hours (Demmig and Winter, 1988; Horton and Hague, 1988). In vascular plants, the fastest and main fraction of *NPQ* is commonly known as "high-energy quenching" qE and relates to the exciton lifetime in the antenna and, thus, to the down-regulation of excitation transfer to photosystems (Gilmore et al., 1998). qE is induced by the ΔpH and is facilitated by the PsbS thylakoid protein (Li et al., 2004); it readily relaxes upon collapse of the ΔpH in darkness. However, qE is also strongly modulated by the reversible de-epoxidation of violaxanthin to zeaxanthin (see for review Demmig-Adams et al., 2014). The *NPQ*-zeaxanthin relationship is uniform among higher plant species (Demmig-Adams and Adams III, 1996), but qE kinetics does not match with zeaxanthin formation/reconversion (reviewed by Jahns and Holzwarth, 2012) and is rather influenced by the zeaxanthin amount retained in darkness (reviewed by Demmig-Adams et al., 2012). Therefore, it is particularly complex, if not impossible, to discern individual mechanisms only based on fluorescence studies, because many mechanisms, widely varying in their onset and relaxation kinetics, co-operate in generating *NPQ*.

Beside qE, other PSII fluorescence quenching components can be recognized in fluorescence terms. The very slowly relaxing qI reflects PSII photoinhibition, whose original definition is "*sustained depressions* in PSII efficiency – irrespective of their nature and mechanism" (Demmig-Adams et al. 2012). Such mechanisms include energy dissipation in photodamaged PSII (Aro et al., 1993), but also other forms of sustained thermal dissipation in the antenna (Jahns and Miehe, 1996; Verhoeven et al., 1996; Dall'Osto et al., 2005; Nilkens et al., 2010). More debated is the role, if any, of state transitions in *NPQ*. Such short-term energy conserving responses are involved when PSI and PSII are unequally excited (red *PSII light* or far red *PSI light*), so as to restore the plastoquinone redox poise (see, e.g., Rochaix, 2013). More recently, state transitions have instead been interpreted as a system to regulate energy distribution between PSI and PSII

under fluctuating natural white light (Tikkanen et al., 2006; Tikkanen and Aro, 2014). Although an enhanced functional association of LHCII to PSI instead of PSII (so-called *state 2* condition) is not properly a dissipative process, it was proposed to result in a measurable fraction of *NPQ*, termed "state-transition quenching" qT, which is biochemically related to the phosphorylation of LHCII and is especially relevant under low-light conditions (Demmig and Winter, 1988; Horton and Hague, 1988; Quick and Stitt, 1989). A reduced antenna cross-section of PSII, resulting from the functional association of a fraction of LHCII with PSI, should cause a decrease in the maximum fluorescence of PSII. This process would be reversible in about ten min of darkness and, therefore, would give rise to an *NPQ* component separated from the faster decaying qE (ca. 1 min). Based on decay time, qT would also be easily distinguished from the nearly irreversible qI. While the increase in PSI antenna size from dark to growth light is a well-established phenomenon facilitated by LHCII phosphorylation (e.g., Goldschmidt-Clermont and Bassi, 2015), it has been repeatedly questioned how much the middle-relaxing component of *NPQ* can reliably reflect the occurrence of this process (see Kalaji et al., 2014 pp. 133-134). In angiosperms, a possible multi-componential origin was suggested, in particular to explain the persistence of qT under high light (Walters and Horton, 1991, 1993; Lokstein et al., 1993). In fact, the previously mentioned limitations in linking fluorescence kinetics with underlying mechanisms appear particularly insidious with respect to qT. Evidence exists indeed both in favor and against an involvement of LHCII phosphorylation, thermal dissipation by slowly-relaxing process(es) and chloroplast photo-relocation for light avoidance (Walters and Horton, 1993; Lokstein et al., 1993, 1994; Nilkens et al., 2010; Joliot and Finazzi, 2011; Cazzaniga et al., 2013). An incomplete closure of PSII during the saturating pulses, caused by the activation of FNR at the acceptor side of PSI, could be another explanation for qT (Schansker et al., 2006).

When an angiosperm's leaf is exposed to high light, the amplitude of qT changes negligibly or even decreases as compared to low light conditions (Quick and Stitt, 1989; Schansker et al., 2006; Ferroni et al., 2014). This observation is in line with the original attribution of qT to state transitions, because it parallels a decline in LHCII phosphorylation promoted by a highly reduced state of stromal thioredoxins (Rintamäki et al., 2000). Indeed, LHCII dephosphorylation under high light could prevent potential energy losses in PSII

upon a subsequent shift to low light (Mekala et al., 2015). At the same time, under high light both photosystems can benefit from the photoprotection allowed by qE generated in the quenched interspersed LHCII lake (Tikkanen and Aro, 2014). The concept of LHCII antenna sharing for protection of both photosystems though qE very likely holds true also for lycophytes, but in these plants - and contrasting to euphyllophytes - qT is also clearly enhanced under high light (Ferroni et al., 2014). This "extra-qT" of lycophytes would be activated by a high-light-induced phosphorylation of Lhcb6, the protein forming the minor antenna CP24 of PSII. Phosphorylation of Lhcb6 seems to be unique to lycophytes, as is also its unprecedented biochemical affinity for PSI (Ferroni et al., 2014). Consequently, the extra-qT of lycophytes could reflect the use of PSI as an energy quencher for PSII through an energy spillover mechanism (Ferroni et al., 2014, 2016). Interestingly, energy spillover to PSI was suggested to be functionally relevant in angiosperms as well, in particular when the light intensity becomes so high that the plant's capacity for qE is saturated and, therefore, insufficient for an effective photoprotection (Tikkanen and Aro, 2014; Yokono et al., 2015; Tiwari et al., 2016).

In this study, we used *Selaginella martensii* to obtain novel insights into the nature of the middle-relaxing component of *NPQ* in a living representative of lycophytes. Based on previous results (Ferroni et al., 2014, 2016), the hypothesis orienting from our work was that the extra-qT reflects a PSI-based mechanism activated in response to a high-light stress. First of all, we analyzed *NPQ* and its kinetic components as a function of irradiance, in order to find out whether the extra-qT can be separated from the ordinary qT. Then, we addressed the following questions about the extra-qT:

a) is the extra-qT induced when irradiance exceeds a certain threshold, corresponding to the saturation of qE and carbon fixation capacity?
b) Under high-light conditions dominated by qE, is the induction of the extra-qT accompanied by a parallel, measurable energy spillover to PSI?
c) Can the induction of the extra-qT be related to an enhanced phosphorylation of Lhcb6, specifically induced under high light?

These questions were addressed using a correlative approach to combine results from fluorescence quenching analysis, gas exchange measurements, emission spectrofluorimetry, and protein phosphorylation detection.

2. Materials and Methods

2.1 Plant material

For the experiments, *Selaginella martensii* Spring (Lycophyta, Selaginellaceae) plants were used. Plants were grown individually in pots in a humid greenhouse of the Botanical Garden of Ferrara, Italy, at 25-30°C under a natural shade light regime. The irradiance of photosynthetically active radiation (PAR) was ca. 70 µmol m^{-2} s^{-1} at the middle of the photoperiod. Data were collected between March and September of several years (2009-2017). More information about photosynthetic properties of *S. martensii* grown under the same conditions is reported in Ferroni et al. (2016).

2.2 Modulated chlorophyll fluorescence

For Chl fluorescence analysis, an ADC OS1-FL PAM fluorometer was used (ADC Bioscientific Ltd, Hoddesdon, UK). After a dark incubation period of at least 30 min, the branches were detached and firmly positioned under the fluorescence probe using a sample clip. The dark-acclimated state was characterized through the basal fluorescence F_0 immediately followed by a saturation pulse of 0.8 s to determine the maximum fluorescence F_M. Subsequently, actinic white light of known irradiance (50-1600 µmol m^{-2} s^{-1}), generated by a halogen lamp, was driven to the sample with fiberoptics in order to generate fluorescence induction kinetics applying a saturation pulse series for 10 min and obtaining the fluorescence values at time *t* (F_t) and the maximum fluorescence F_M'. The F_0' value of the minimum fluorescence in the light-exposed sample was evaluated using the equation proposed by Oxborough and Baker (1997). After the induction, the dark relaxation kinetics was followed applying a series of pulses for 40 min. Photochemical quenching $qP=(F_M'-F_t)/(F_M'-F_0')$ (van Kooten and Snel, 1990) and non-photochemical quenching $NPQ=(F_M-F_M')/F_M'$

determined at the end of the induction period were plotted against the irradiance to generate light-response curves.

The dark-relaxation kinetics of fluorescence was used to resolve *NPQ* components differing in their decay time, starting from the original method described by Walters and Horton (1991) as detailed in Appendix A. In a log(*NPQ*)-time diagram in which the components that decay exponentially linearize, the fastest component is ascribed to the qE; once qE has relaxed, the decay of *NPQ* reveals the presence of a slower component qT, up to leaving the residual fraction qI, which does not relax in the experimental dark period. In the general case, amplitude and kinetics properties of qE and qT were resolved by fitting the relaxation curves with the combination of two exponential decays and a constant (qI) (Ferroni et al., 2016). However, in the cases in which the relaxation of qT was visibly affected by a delay, the analytical procedure was simplified because of the clear temporal separation of qE and qT. The values obtained for each component were used to generate light-response curves.

2.3 CO_2 exchange

CO_2 exchange was measured in terminal braches with an LCA-4 infrared gas analyzer (ADC Bioscientific Ltd, Hoddesdon, UK). The dark respiration values were obtained by wrapping the measuring chamber with aluminum foil; then the sample was exposed to an increasing irradiance series. The light source was a set of halogen lamps screened by a 4-cm-thick layer of water. After the measurement, the analyzed branch was excised and its surface area was measured to normalize the gas exchange on an area basis for determination of the net photosynthesis, as net CO_2 uptake (*A*). The irradiance-*A* curves were fitted according to Peek et al. (2002), using the following non-linear function:

$$A = A_{max}\left[1 - e^{-k(I-LCP)}\right],$$

where I is incident irradiance, A_{max} is the asymptote of photosynthesis at high light and corresponds to the light saturated *A*, *LCP* is the irradiance at the light saturation point, and *k* is initial slope corresponding to the apparent quantum yield of CO_2 fixation. As an estimate of the irradiance of saturation, the equation

was resolved for the *A* value corresponding to 95% of A_{max}. Curve fitting was performed with OriginPro 2015 (OriginLab Corp., Northampton, MA, USA).

2.4 *Steady-state low temperature spectrofluorimetry*

Detached leaves, immersed in an aqueous solution of glycerol 80% (v/v) in a quartz capillary, were illuminated through an artificial sun lamp (Fiber-Lite DC-950 - Dolan-Jenner Instruments), equipped with a Liquid Light Guide (Newport 77568). Light treatments were provided for 10 minutes at 50, 100, 200, 400, 800, 1600 µmol m^{-2} s^{-1}. The light intensity was measured by the light meter QRT1 Quantitherm (Hansatech Instruments).

Low temperature (77 K) emission and excitation spectra were registered using a LS55 spectrofluorimeter (Perkin Elmer), equipped with a red sensitive photomultiplier and a low temperature capillary holder. The emission spectra were measured by scanning from 640–800 nm, using an excitation light set to 436 nm (targeted at Chl *a* absorption maxima). The Gaussian deconvolution of the normalized emission spectra was done with OriginPro 2015 software for components having peaks at 670, 679.5, 685, 694, 701, 714, 735 nm and a vibrational band at ca. 760 nm (Ferroni et al., 2009). Excitation spectra were measured by scanning from 400–520 nm with an emission wavelength of 730 nm. The spectral bandwidth was 10 nm (excitation) and 10 nm (emission).

2.5 Steady-state room temperature spectrofluorimetry

For analysis of steady-state fluorescence emission, terminal branches were cut from overnight dark-acclimated plants and allowed to float on 20 mM NaF for 1 h in order to prevent unwanted protein dephosphorylation during sample manipulation. Subsequently, the branches were light-treated for 15 min. Single leaves were then sampled and mounted in water on microslides to record room-temperature fluorescence emission spectra with an epifluorescence microscope (Carl Zeiss, Oberkochen, Germany) equipped with a microspectrofluorimeter (RCS, Firenze, Italy; Pancaldi et al., 2002; Ferroni et al., 2011). Excitation at 436 nm was driven to small cell groups of the upper leaf epidermis using a using a 1.6 mm diaphragm in combination with a Zeiss Plan-Neofluar 40×. Fluorescence emission was collected in the 620-

780 nm range and the spectra were elaborated using OriginPro 2015. In detail, spectra were double normalized and the emission intensity in the PSI region was determined by curve integration between 710 and 750 nm.

2.6 Analysis of thylakoid protein phosphorylation

The terminal branches were sampled from plants just after the night (dark-acclimated state) or after 1 h exposure to the light provided by halogen lamps screened by 4 cm of water (50-1600 µmol m^{-2} s^{-1} PAR; Ferroni et al., 2016). After the light treatment, the terminal branches were immediately excised and subjected to thylakoid isolation essentially according to Järvi et al. (2011) and Ferroni et al. (2016), having added 10 mM NaF to all buffers to inhibit the phosphatases (Rintamäki et al., 2000). Chl content in the thylakoid samples was determined spectrophotometrically after extraction with 80% aqueous acetone (Porra et al., 1989). To analyze the steady-state phosphorylation of thylakoid proteins, SDS-PAGE of thylakoid proteins was performed on a resolving gel with 15% acrylamide and 6 M urea (Laemmli, 1970). Subsequently, thylakoid phosphoproteins were detected by immunoblotting on nitrocellulose or poly(vinylidene difluoride) membrane, using antibodies raised against phosphothreonine (Zymed or New England Biolabs) and a detection system based on enhanced chemiluminescence or chromogenic reactions. The same protocols were used to detect the D1 protein of PSII reaction center (Agrisera???).

Band intensity was analyzed with ImageJ freeware (National Institutes of Health, Bethesda, MD, USA). In order to make all tests comparable with each other and allow an easier comparison of LHCII and Lhcb6 phosphorylation levels, the values obtained for each protein were double normalized between 0 (minimum signal) and 1 (maximum signal) and then averaged. The double normalization procedure is presented in more detail in Supplementary Fig. 1.

2.7 Statistical data treatment and graphical representation

Statistical analyses were performed with OriginPro 2015. Correlation between variables was checked after a linear regression, whose significance was tested by ANOVA using a threshold of $P<0.05$. The same

software was used for the graphical representations, connecting mean data points through the built-in functions.

3. Results

3.1 Irradiance dependence of NPQ components

Our starting hypothesis was that, in the lycophyte *S. martensii*, the middle phase in *NPQ* relaxation, which we termed qT for consistency with the previous literature, could include an extra-qT component due to a mechanism(s) specifically induced under a high-light stress (Ferroni et al., 2014). To this aim, the light-dependency of *NPQ* and its kinetic components was analyzed to cover irradiance values from close to growth light (50-100 µmol $m^{-2}s^{-1}$) to largely exceeding growth light (up to 1600 µmol $m^{-2}s^{-1}$). All *S. martensii* plants used for experiments were grown under stable natural shade conditions and, therefore, had never experienced irradiances ≥200 µmol $m^{-2}s^{-1}$ before experiments. *NPQ* induction kinetics under each independent irradiance level was followed for 10 min. In each case, *NPQ* was strongly induced within the first min, reflecting the prompt creation of the trans-thylakoid ∆pH (Tikhonov, 2015). For irradiance values ≤ 200 µmol $m^{-2}s^{-1}$, *NPQ* then declined to lower steady-state values, corresponding to the activation of the downstream use of ATP (Joliot and Finazzi, 2010; Tikhonov, 2015) (Fig. 1a). At higher irradiances, the initial rise in *NPQ* was instead followed by a further slower moderate increase. The *NPQ* values reached at the end of the induction period were used to build the light curve shown in Fig. 2a.

NPQ is recognized as the result of a composite of processes, each capable to quench F_M. After each light induction, the F_M' was allowed to recover in darkness for 40 min to resolve *NPQ* components differing in their decay time. The decay of *NPQ* was better visualized by plotting *NPQ* values in a logarithmic scale against time, as shown in Fig. 1b. Based on literature data, over a period of 40 min, *NPQ* relaxation was expected to occur through three phases: a fast phase (qE, decay time < 1 min), a middle phase (qT, decay time ca. 10 min) and a very slow phase (qI, decay time of hours) (Guadagno et al., 2010). The original subtractive approach used by Walters and Horton (1991) to resolve the amplitude of each component implicitly presupposes that all *NPQ* components start their decay at time 0, as soon as the actinic light is

turned off, so that the relaxation curve can be treated as the sum of two exponential decay curves (qE and qT) and a constant, which approximates the nearly unrelaxable fraction (qI). For each tested irradiance, the first fast decaying qE component was obviously evident (Fig. 1b). Conversely, there were two possibilities for the transition to the slower phases (Fig. 1b insert). In relaxation tests after low-medium irradiance (<400 µmol $m^{-2}s^{-1}$), there was a ca. 2 min-long lag in the decay of qT, in fact the relaxation of qE was followed by plateau values of *NPQ* before *NPQ* decreased further. In these cases, the two segments of the curve were fitted separately, each with an exponential function. At higher irradiance, the relaxation curves adequately matched the model and curves were fitted accordingly. Results of the fitting procedure are reported in Table 1 and the amplitudes of the three *NPQ* components were used to generate as many light curves (Fig. 2).

Table 1. Kinetic properties of *NPQ* components resolved from *NPQ* relaxation in *Selaginella martensii*.

Irradiance (µmol m^{-2} s^{-1})	*decay time* τ		*half time*		*Amplitude* A		
	qE (s)	qT (min)	qE (s)	qT (min)	qE	qT	qI
50	22.6 ± 3.3	9.07 ± 2.09	15.7 ± 2.3	6.29 ± 1.45	0.14 ± 0.05	0.10 ± 0.02	0.037 ± 0.036
100	26.2 ± 4.7	11.31 ± 0.84	18.2 ± 3.2	7.84 ± 0.58	0.75 ± 0.08	0.15 ± 0.03	0.004 ± 0.006
200	20.5 ± 2.2	10.21 ± 2.56	14.2 ± 1.5	7.08 ± 1.78	1.34 ± 0.06	0.15 ± 0.03	0.022 ± 0.016
400	18.1 ± 2.1	10.96 ± 3.13	12.5 ± 1.5	7.60 ± 2.17	2.03 ± 0.14	0.20 ± 0.05	0.07 ± 0.02
800	21.4 ± 2.4	13.58 ± 4.49	14.8 ± 1.6	9.41 ± 3.11	2.51 ± 0.22	0.27 ± 0.05	0.13 ± 0.04
1600	26.0 ± 5.6	11.27 ± 3.60	18.0 ± 3.9	7.81 ± 2.50	2.82 ± 0.31	0.35 ± 0.12	0.18 ± 0.07

Plants were exposed to 10 min light of known irradiance to induce NPQ and allowed to relax in darkness for 40 min. Data were obtained through an exponential decay fitting of relaxation curves (see Fig. 1b and Appendix A) and reported as means of N = 3 ± SD. Decay time of qE and qT were analyzed with ANOVA yielding non-significant differences between irradiance treatments. Amplitude values were used to draw graphs in Fig. 2.

qE was the main component of *NPQ*. The qE-light curve was similar to that of *NPQ*, except for a more pronounced sigmoidicity (Fig. 2a). This last aspect depended on a higher contribution of non-qE components to *NPQ* at 50 µmol $m^{-2}s^{-1}$ (in particular qT, see Fig. 2b) and on a more marked tendency of qE

to saturate at the highest irradiances. The light curve of qT amplitude revealed that the induction of a qT component of *NPQ* already occurred at 50 µmol $m^{-2}s^{-1}$ and increased with the irradiance (Fig. 2b). In particular, qT increased almost steadily over the whole range of irradiances and did not saturate. At the highest irradiance qT accounted for 10% of *NPQ*. The characteristic decay time was of ca. 10-11 min (corresponding to a half-time of ca. 7-8 min) and was independent of the irradiance previously used for induction (Table 1).

Having obtained the light-dependency of qT and qE, we tested analytically the hypothesis that in *S. martensii* the induction of qT would become more relevant when the light irradiance exceeds a threshold corresponding to the saturation of the plants' capacity for qE (Ferroni et al., 2014). In a graphical analysis, this means that the amplitude of qT should increase asymptotically when the saturation value of qE is approached, thus indicating the possible occurrence of a specific "high-light qT" component. In the qT *vs* qE plot of Fig. 2c, qT was induced at a certain level until qE reached a value of 1.5, and then for qE>1.5 a further induction of qT occurred. We assumed this last component to be the extra-qT, already induced at irradiance values that only moderately exceeded that of growth (>200 µmol $m^{-2}s^{-1}$).

The residual photoinhibitory qI fraction of *NPQ* was absent or completely negligible just up to and including 200 µmol $m^{-2}s^{-1}$, and then rose, closely paralleling the extra-qT (Fig. 2b). At the highest irradiance qI accounted for <5% of total *NPQ*. From a comparison between qT and qI trends, extra-qT was induced at the onset of PSII photoinhibition, as shown by their linear relationship limited to the range of 200-1600 µmol $m^{-2}s^{-1}$ (Adj. R^2 = 0.980 with $P < 0.01$; Fig. 2d).

3.2 Correlation of qT with the excitation energy pressure inside PSII

The F_M quenching analysis suggested that the mechanism underlying the extra-qT could be activated when PSII is exposed to potentially photoinhibiting light intensity. The probability for PSII to be inactivated primarily depends on the reduction state of the plastoquinone pool, which determines the steady state fraction of closed PSII centres. Taking into account the recommendations in Kalaji et al. (2016, pp. 22-23), the photochemical quenching was calculated as qP (open PSII) and its complement to unity 1-qP (closed

PSII) was used to obtain an estimate of the excitation energy pressure inside PSII (Ögren and Rosenqvist 1992; Björkman and Demmig-Adams, 1995). qP focuses the analysis on the PSII population which can do a photochemical charge separation, i.e., excludes the PSII centers not reached by excitons because of non-photochemical quenching. Namely, qP measures the position of F_t in a scale comprised from F_0' (all Q_A oxidized) to F_M' (all Q_A reduced). In *S. martensii*, 1-qP sharply rose from 0 to 100 µmol $m^{-2}s^{-1}$, but a further increase to 200 µmol $m^{-2}s^{-1}$ did not result in an increment in excitation energy pressure. For irradiances >200 µmol $m^{-2}s^{-1}$, 1-qP increased again reaching a plateau level at 800 µmol $m^{-2}s^{-1}$ (Fig. 3a). It was found that qT was linearly correlated with 1-qP, indicating that the amplitude of qT was linked to the excitation energy pressure inside PSII (Adj. R^2 = 0.864 with $P < 10^{-2}$). However, 1-qP saturated at irradiance >800 µmol $m^{-2}s^{-1}$, while qT did not. In fact, the correlation became more significant when the irradiance of 1600 µmol $m^{-2}s^{-1}$ was excluded from calculation (Adj. R^2 = 0.938 with $P < 10^{-3}$; Fig. 3b).

Excitation energy pressure inside PSII is, among other factors, the reflection of the carbon fixation ability of a plant (see Maxwell and Johnson, 2000; Kalaji et al., 2014). In order to obtain further elements to interpret the fluorescence quenching results, light curves of steady-state net photosynthesis (*A*) were recorded (Fig. 3a). At saturation, A_{max} was of only 1.53 ± 0.35 µmol CO_2 $m^{-2}s^{-1}$, lower than usual for shade plants (around 5-8 µmol CO_2 $m^{-2}s^{-1}$). The apparent quantum yield for CO_2 fixation was of k = 0.020 ± 0.005 and the light compensation point was found at 31.6 ± 8.3 µmol $m^{-2}s^{-1}$, while the irradiance resulting in 95% of A_{max} was 196 ± 38 µmol $m^{-2}s^{-1}$. At the irradiance of 800 µmol $m^{-2}s^{-1}$ a decline of *A* towards values <A_{max} indicated an incipient measurable effect of photoinhibition on carbon fixation. Therefore, from the comparative view of *A*, 1-qP, and qT trends shown in Fig. 3a, the extra-qT was induced when *S. martensii* sensed the increase in PSII excitation energy pressure caused by the saturation of the dark reactions of photosynthesis.

3.3 qT and antenna redistribution to PSI

According to its original interpretation, the changes in qT should reflect similar variations in antenna redistribution from PSII to PSI. We investigated this aspect recording low temperature fluorescence

emission spectra *in vivo* from leaves. A quite low relative PSI emission at 77 K is consistent with the low PSI/PSII ratio in this species acclimated to understory shade (see Ferroni et al., 2016; Fig. 4a). Fig. 4a shows that treatments with increasing irradiance resulted in a more and more intense relative emission from PSI, peaking approximately at 730 nm. Since spectra were normalized to PSII emission at ca. 685 nm, an increase in relative PSI emission under high light could be ascribed to an enhanced energy transfer to PSI and/or to a decrease in PSII emission caused by photodamage. To test whether a larger antenna pool was serving PSI, excitation spectra were recorded at 730 nm, in fact relative variations in Chl *b* excited emission are diagnostic for energy transfer from LHCII (Ruban et al., 2006; Tikkanen et al., 2008). As compared to dark-acclimated samples, the excitation peak of Chl *b* (480 nm) was enhanced not only in leaves acclimated to low light (100 µmol m^{-2} s^{-1}), but even more in those treated with the highest irradiance of 1600 µmol m^{-2} s^{-1} (Fig. 4b). Conversely, immunoblot detection of D1 protein of PSII reaction center excluded a major effect of PSII photodamage in determining the relative gain in PSI emission (Fig. 4c). Therefore, the strong increase in PSI relative emission was primarily due to more excitation energy reaching PSI through the LHCII antenna system, resulting in a more and more pronounced *state 2*-like condition for ever increasing irradiance levels.

PSI fluorescence emission arises from different sources (Croce et al., 1997). We deconvoluted the 77 K emission spectra into Gaussian components, in particular in the PSI region two contributions were resolved, F714, corresponding to *red Chls* of PSI core, and F735, emitted by *red Chls* in PSI-LHCI complexes (see references in Kalaji et al., 2017, pp. 31-33). Examples of deconvoluted spectra are shown in Fig. 5a-c and correspond to representative dark-acclimated condition (*state 1*), low light-acclimated condition (*state 2*), and high light-acclimated condition. In spite of sharing a generally increasing trend, the light-dependency of F714 and F735 were markedly different (Fig. 5d). In fact, the transition from darkness to low light had a much stronger impact on F735 (+85%) than on F714 (+25%), while F714 increased more upon exposure of leaves to higher irradiance (Fig. 5d). This was distinctly seen with the F735/F714 ratio, showing a peak under low-moderate light and then a decline (Fig. 5e). Existence of a linear relationship between qT and F714 was clearly evident all over the analyzed irradiance range and was confirmed by regression

analysis (Adj. R^2 = 0.941 with $P < 10^{-3}$; Fig. 5f). Differently, data distribution of qT *vs* F735 suggested a more complex non-linear relationship between these variables (Fig. 5g).

3.4 qT strongly correlates with the phosphorylation level of Lhcb6, but not of LHCII

Results from 77K emission spectroscopy prompted us to analyze the primary mechanism enhancing energy transfer to PSI, i.e., phosphorylation of LHCII, which follows a repeatedly reported light-intensity dependent behavior (Demmig et al., 1987; Rintamäki et al., 2000; Rantala et al., 2016). In lycophytes, it is complicated by the phosphorylation of Lhcb6, which should specifically occur in response to high light (Ferroni et al., 2014). *S. martensii* plants were exposed to increasing irradiance and the thylakoid phosphoproteins were analyzed at the steady state. The thylakoid phosphoproteins detected with an anti-phosphothreonine antibody in *S. martensii* matched those previously identified by Ferroni et al. (2014). In Fig. 6a the model angiosperm *Arabidopsis thaliana* was included for reference. Both species showed phosphorylation of the PSII core proteins D2 and CP43, as well as of proteins belonging to the major LHCII. *S. martensii* did not phosphorylate the D1 protein of PSII, as known for seedless plants (Pursiheimo et al. 1998), but showed the additional phosphoprotein Lhcb6 (Ferroni et al., 2014). The lowest levels of protein phosphorylation were found in the dark-acclimated samples, and exposure to light increased the phosphorylation of the PSII core proteins (Tikkanen et al., 2006; Grieco et al., 2012; Wientjes et al., 2013b). The phosphorylation trends of the major LHCII and Lhcb6 were clearly different from each other. Fig. 6b compares relative phosphorylation changes of LHCII and Lhcb6, after a procedure of double normalization between minimum and maximum levels (see Supplementary Fig. S1). Phosphorylation of LHCII rose to its maximum at 100 µmol $m^{-2}s^{-1}$, and then progressively decreased to little more than the dark value when the plants were exposed to 800 µmol $m^{-2}s^{-1}$. A new increase occurred under the highest irradiance used in experiments, i.e. 1600 µmol $m^{-2}s^{-1}$. Phosphorylation of Lhcb6 was induced in parallel to that of LHCII up to an irradiance of 200 µmol $m^{-2}s^{-1}$, but, contrastingly, for higher values it further increased up to saturation at 800-1600 µmol $m^{-2}s^{-1}$.

Interestingly, the phosphorylation trend of Lhcb6 was strikingly similar to the light curve of qT, except for the fact that Lhcb6 phosphorylation saturated, while qT did not. In the range of 0-800 µmol $m^{-2}s^{-1}$ the correlation between Lhcb6 phosphorylation and qT was significant with $P < 10^{-2}$ (ANOVA, Adj. R^2 = 0.969; if the intercept was set at the origin of axes, Adj. R^2 = 0.998 with $P < 10^{-5}$) (Fig. 6c).

3.5 qT and energy transfer to PSI at physiological temperature

While it was clear that antenna association with PSI occurred in *S. martensii* under increasing light, it remained to evaluate whether such *state 2*-like condition had any importance at physiological temperatures, when most excitons are actually dissipated in the antenna before reaching either PSII or PSI because of qE (Tikkanen and Aro, 2014). At physiological temperature, fluorescence emitted from PSI *red Chls* is strongly quenched as compared to 77 K, because they can transfer energy to the P700 (reviewed by Itoh and Sugiura, 2004), which finally quenches excitation independent of its redox state (Schlodder et al., 2005). However, a small fraction of excitation energy is still emitted as fluorescence, whose intensity will depend on the amount of energy that *red Chls* can accumulate. If in *S. martensii* under increasing light the role of LHCII/Lhcb6 association with PSI is to quench excitation *before* it reaches PSI, emission from *red Chls* will change negligibly. Conversely, if its role is to drive excitation up to P700, more energy will stabilize at *red Chls* traps, increasing their fluorescence emission. To possibly discern between these two options, steady-state fluorescence emission spectra were recorded at room temperature. Analysis was circumscribed to the only upper epidermal chloroplasts, i.e., those also probed by PAM fluorescence. Similarly to 77K spectra, PSI is responsible for fluorescence emission in the long wavelength region above 700 nm. That self-reabsorption of emitted light, which tends to increase emission in the PSI region (Franck et al., 2002), is negligible when using microspectrofluorimetry (Ferroni et al., 2011). Furthermore, in the hypothesis of an involvement of antenna protein phosphorylation, the dark-acclimated samples were pre-incubated in darkness with NaF to limit protein de-phosphorylation during sample preparation and analysis.

Fig. 7a compares the normalized average spectra obtained from dark-acclimated samples or after exposure to 100, 200 or 1600 µmol $m^{-2}s^{-1}$. For an approximation of PSI emission, the area subtended under

the curve between 710 and 750 nm was used, so as to minimize the contribution by the PSII vibrational satellite (>750 nm). This approach was used as a good compromise between an analysis at single wavelength (e.g. 730 nm; Ferroni et al., 2016), which is very simple but overlooks the complex origin of fluorescence emission in PSI and LHCI, and spectra deconvolution, which can resolve individual PSI-LHCI emitters, but suffers from resolution uncertainty because of overlapping PSII broad side bands (Ferroni et al., 2011). The light dependence of the relative PSI emission revealed two easily distinguishable light-ranges in which a preferential energy distribution to PSI occurred. In particular, starting from 0 to 100 µmol $m^{-2}s^{-1}$, PSI emission sharply increased to its maximum, reflecting the transition from the dark-acclimated state (*state 1*) to the growth-light acclimated state (*state 2*) (Wientjes et al., 2013b; Fig. 7b). An increase in irradiance caused an evident decline in PSI relative emission and, more in general, an increased peakedness of spectra. However, when light became more intense, a linear, progressive rise in PSI emission occurred (Fig. 7b). Consequently, the relationship between PSI emission and qT was not obvious, as shown in the qT *vs* PSI emission plot of Fig. 7c. The irradiance range corresponding to the ordinary qT yielded a linear correlation between 0 and 100 µmol $m^{-2}s^{-1}$ (Adj. R^2 = 0.996 with $P < 0.05$), but noticeably qT failed to reveal the drop in PSI emission at 200 µmol $m^{-2}s^{-1}$. Conversely, an independent linear correlation was found in the irradiance range of the extra-qT (Adj. R^2 = 0.931 with $P < 0.05$).

Interestingly, spectra recorded under either 100 or 1600 µmol $m^{-2}s^{-1}$ were quite similar to each other. This was better seen comparing the profiles of the difference spectra calculated with respect to the dark-acclimated samples, as shown in Fig. 7d: in both cases, an increase in PSI emission (720-730 nm) occurred at the expense of PSII emission (689 nm). Control experiments were performed to evaluate potential side effects on PSII integrity caused by the general inhibition of phosphatases brought about by NaF (Supplementary Fig. S2). NaF disturbance of phosphorylation-dependent PSII repair (reviewed in Järvi et al., 2005) did not have any appreciable impact on the PSII emission region under our experimental conditions. Therefore, the main effect of NaF was to lock-in the antenna in the light-induced phosphorylated state, which favors energy transfer to PSI. Finally, difference spectra revealed a gain at 677 nm, specific to the 1600 µmol $m^{-2}s^{-1}$ samples, attesting the presence of free LHCII under high light (Pantaleoni et al., 2009).

4. Discussion

Beside the dominating and most studied fast inducible/relaxable qE, the existence of a kinetic component of *NPQ* relaxing in some ten min has been known for decades and is termed qT after its early attribution to state transitions (Demmig and Winter, 1988; Horton and Hague, 1988; Quick and Stitt, 1989; Hodges et al., 1989). Nevertheless, its mechanistic nature and significance for photoprotection are still controversial. The present study moves from the hypothesis that in lycophytes the qT induced under high light could be separate from the ordinary qT activated at low light. In *Selaginella martensii*, qT is promptly induced to a steady-state value upon exposure to low-medium light intensity, but shows indeed a further increment under high light (Fig. 1b).

Based on the close relationship between qT and *1-qP*, it is clear that the mechanistic processes responsible for qT are activated in response to the excitation energy pressure inside PSII and, therefore, can be qualified as regulatory of electron transport (Fig. 3b). The diversity of mechanistic interpretations proposed in angiosperms for qT over the past three decades warns about the assignment of qT to one specific mechanism. As for qE and qI, several processes should be evoked to justify the existence and properties of the *NPQ* component decaying in some 10 min (Lokstein et al., 1993). Therefore, in the lycophytes *S. martensii* as well, qT and extra-qT are measurable physical variables that very likely depend on a combination of mechanisms, which we have tried to dissect in this work. It was previously shown that, in *S. martensii* under high light, the extent of qT is somewhat related to the relative content of PSI and FNR (Ferroni et al., 2016). Therefore, among different alternatives, a photochemical quenching of F_M by downstream electron flow from PSI through FNR is an interesting possibility for qT (Schansker et al., 2006). It has the advantage of providing an explanation for the ca. 2 min-long delay in qT relaxation (i.e., the time required for the dark-inactivation of FNR; Schansker et al., 2006), which is more clearly observed in *S. martensii* after induction with low-medium irradiance (Fig. 1b). However, this hypothesis anticipates as well that the extent of qT should be nearly independent of irradiance (Schansker et al., 2006), whereas in *S. martensii* we demonstrate an obvious increasing trend when light exceeds saturation (Fig. 2b). Therefore,

while FNR activation state can represent the “on/off” switch for qT to occur, the extent of qT must depend on other mechanisms tuned on light intensity. In particular, the close relationship between qT and F714 strongly implicates the involvement of a regulatory PSI-based mechanism.

Induction of qT occurs already in the range of light limitation, reaching stable values in the early CO_2-limited phase (<200 µmol $m^{-2}s^{-1}$). In angiosperms, one main reason for interpreting qT as a state-transition quenching was the parallel rise of qT, energy distribution to PSI, and LHCII phosphorylation under low light (Walters and Horton, 1993). The classical model of state transitions was elaborated to interpret the response to changes in spectral quality of light, i.e, “pushing the system towards its extremes, state 1 or state 2” (for a comprehensive review, see Goldschmidt-Clermont and Bassi, 2015). However, a state-transition-like process is also known to occur following the shift from the dark-acclimated state to the growth light-acclimated state (Goldschmidt-Clermont and Bassi, 2015). Accordingly, in *S. martensii*, maximum LHCII phosphorylation approximates the irradiance of growth and exactly matches the rise in PSI emission at 77 K, especially F735, as well as at room temperature (Fig. 5d, 6b, 7b). Under growth light conditions, extensive LHCII phosphorylation all over the thylakoid membrane regulates the efficiency through which energy is channeled to PSI and PSII embedded in the LHCII lake (Tikkanen et al., 2006, 2008; Wientjes et al., 2013a, 2013b; Grieco et al., 2015). The fine tuning of energy distribution between PSI and PSII allows a plant to optimize electron transfer and is vital to especially preserve PSI integrity under natural fluctuations in light intensity (Tikkanen et al., 2010; Grieco et al., 2012).

Increase in irradiance from 100 to 200 µmol $m^{-2}s^{-1}$ is counteracted by the induction of qE, which lowers the probability that excitons are transferred to both reaction centres (Fig. 2a; Gilmore et al., 1998; Tikkanen and Aro, 2014; Grieco et al., 2015). Since under “qE conditions” the energy transfer to PSI is promoted (Jajoo et al., 2014; Yokono et al., 2015), in angiosperms an effective management of the absorbed light also includes a decrease in LHCII phosphorylation at this stage. The regulation of LHCII phosphorylation is due to the contrasting activity of STN7 kinase (Bellafiore et al., 2005) and TAP38/PPH1 phosphatase (Shapiguzov et al., 2010; Pribil et al., 2010). The de-phosphorylation of LHCII under high light depends on STN7 inhibition by reduced thioredoxins (Rintamäki et al., 2000) and on TAP38/PPH1

accumulation in PSII-LHCII-PSI megacomplexes (Rantala et al., 2016). Down-regulated LHCII phosphorylation would compensate for the preferential energy transfer to PSI and probably prevents energy losses in PSII, in case the plant is exposed to a sudden decrease in irradiance (Mekala et al., 2015). Therefore, in angiosperms, the overall response to high light results in a decrease in excitation pressure on PSI, because qE excludes a PSI pool from excitation pathways and, at the same time, LHCII de-phosphorylation restores a *state 1*-like condition. In this respect, the behavior of the lycophyte is more complex. On one side, de-excitation through qE is so effective that PSI emission at room temperature declines (Fig. 7b); on the other side, plants still maintain a *state 2*-like condition, which is not reversed by incipient LHCII de-phosphorylation (Fig. 5d, 6b).

A sustained *state 2*-like condition characterizes the response of *S. martensii* to ever increasing irradiance levels in the CO_2-limited phase, when an extra-qT is enhanced in parallel with photoinhibitory qI (Fig. 2b, d). Interestingly, up to 800 µmol $m^{-2}s^{-1}$, increase in 77 K PSI emission and qT occur notwithstanding that LHCII is progressively de-phosphorylated (Fig. 6b). Therefore, a possibility explored in this study was that the increase in PSI emission and the induction of extra-qT could relate to the energy transfer to PSI mediated by phosphorylated Lhcb6 (PLhcb6). While in angiosperms Lhcb6 is involved in light harvesting and energy dissipation for PSII (Passarini et al., 2009), in lycophytes it can also be found in native association with PSI (Ferroni et al., 2014). In *S. martensii*, a relationship between qT and PLhcb6 was previously proposed to explain the persistency of qT under high light and its inhibited relaxation by NaF (Ferroni et al., 2014). Nonetheless, we show that the correlation between qT and PLhcb6 is not limited to the irradiance range leading to extra-qT, but it covers instead *the entire light intensity range*, although it is finally lost at 1600 µmol $m^{-2}s^{-1}$ (Fig. 6c). That the ordinary qT and extra-qT could actually reveal two facets of the same mechanism(s) is also strongly suggested by the meaningful correlation between qT and F714 (Fig. 5d). Under low light, in *S. martensii*, the excitation energy directed from LHCII to PSI is mainly stabilized in LHCI, where *red Chls* emit F735; but, when light becomes more intense, the importance of an alternative route progressively emerges, leading to F714 emission directly from PSI core complex (Fig. 5e; PSI emission bands reviewed by Itoh and Sugiura, 2004). These observations corroborate the concept that plants can exploit

alternative excitation routes to drive excitation from LHCII to PSI (Benson et al., 2015). The process impacting on qT extent is evidently the energy transfer route giving rise to F714, while the relationship with the low-light state transition, enhancing F735, appears weak and quite probably coincidental (Fig. 5f, g). At physiological temperature, PLhcb6-mediated energy transfer to PSI is hidden by prevailing LHCII-mediated state transition under growth light, and then by general qE de-excitation at the saturation light (Fig. 7b). Only when light is exceedingly high, i.e., exactly in the extra-qT range, operation of this route is manifested by increased PSI emission, leading to a *quasi-state 2* condition even detectable at room temperature (Fig. 7d). Since this "qT-F714" route marks out a thylakoid membrane response to very high light, its physiological significance can be better described and understood in terms of energy spillover than of classical state transitions.

A decline in PSII/PSI emission ratio under high light was already known from early studies in angiosperms and was interpreted as a consequence of PSII photoinhibition, whereas energy spillover to PSI was excluded (Walters and Horton, 1991, 1993). Energy spillover to PSI is instead currently considered of great relevance for photoprotection under very high light and its structural basis would be the accumulation of large thylakoid megacomplexes, where PSI and PSII can organize in close proximity to each other (Suorsa et al., 2015; Yokono et al., 2015; Rantala et al., 2017; see also Demmig-Adams et al., 2015; Schumann et al., 2017). Moreover, ever accumulating evidence shows that LHCII can act as an efficient antenna for PSI well beyond the limits of classical state transitions (Wientjes et al., 2013a; Benson et al., 2015; Grieco et al., 2015; Akhtar et al., 2016; Bressan et al., 2016; Bos et al., 2017). A prominent use of PSI as a quencher is not surprising in a lycophyte with very low photosynthetic efficiency, as is *S. martensii*, where PLhcb6 could be permissive with respect to the assembly of the "energy spillover" configuration. A high-light-induced accumulation of PSI-PSII-LHCII megacomplexes was recently demonstrated in *S. martensii* (Ferroni et al., 2016) and could be the structural basis for the energy spillover from PSII to PSI. Noticeably, the increased excitation energy pressure inside PSII results only in a small qI and no remarkable depletion in D1 protein is detected, indicating that PSII photoinhibition is efficiently kept under control (Fig.

2b, 4c). This can just be achieved exploiting the quenching capacity by PSI when thermal dissipation through qE has been almost completely saturated.

Consistent with a photoprotective role, the "exciton sink capacity" of PSI is very high, in fact F714, energy spillover at room temperature and qT are roughly proportional to irradiance and do not saturate within the irradiance range analyzed in this work. Since Lhcb6 phosphorylation cannot be further increased at 1600 µmol $m^{-2}s^{-1}$, *S. martensii* exploits the quenching potential of PSI by phosphorylating again LHCII (Fig. 6a, b). Tiwari et al. (2016) recently reported that LHCII phosphorylation was unusually enhanced under high light in the Arabidopsis mutant *pgr5*, which is impaired in generating the trans-thylakoidal ΔpH and, consequently, in inducing *NPQ* (Munekage et al., 2002; Suorsa et al., 2012). This LHCII phosphorylation occurs following the damage of FeS clusters in PSI caused by an uncontrolled electron transfer to PSI, which results in a chronic PSI acceptor side limitation (Tiwari et al., 2016). Through LHCII phosphorylation, the mutant maximizes energy transfer to, and dissipation by, damaged PSI; energy transfer route from LHCII to PSI specifically results in enhanced emission from PSI core, not LHCI (Tiwari et al., 2016). By analogy, we suggest that in *S. martensii*, under extremely high light, the extent of energy transfer to PSI is cooperatively regulated by Lhcb6 and LHCII phosphorylation, which could together participate in determining the level of F714 and qT. However, the condition of *S. martensii* is not exactly equivalent to that of the *pgr5* mutant. In fact, the lycophyte was proven to be very effective in controlling the acceptor side limitation of PSI (Ferroni et al., 2016). Conversely, the phosphorylation of LHCII/Lhcb6 can be related to the safe non-photochemical dissipation of excess energy in donor-side limited PSI ($P700^+$-containing centres), whose fraction was previously shown to be constant over the entire carbon-limited range (Ferroni et al., 2016). The cooperation of LHCII and Lhcb6 in diverting energy from PSII to PSI can find an interesting counterpart in the preferential association of PLhcb6 with free LHCII trimers in a free LHCII/Lhcb6 assembly complex (Ferroni et al., 2014). More in general, under such harsh conditions, the gain in emission at 677 nm testifies to a generalized release of free antenna complexes as a main event occurring in the thylakoid membrane (Fig. 7d; van der Weij-de Wit et al., 2007; Baldisserotto et al., 2013). The release of free LHCII certainly results in a reduced efficiency of energy transfer to PSII (Bielczynski et al., 2015); however, based on the in

vitro competence of LHCII to interact with PSI (Akhtar et al., 2016), it cannot be excluded that the LHCII trimers/assembly complexes also participate in promoting energy transfer to PSI.

5.1 Conclusions

The use of PSI as a safe excitation quencher for PSII is a debated, emerging issue about thylakoid photoprotection in angiosperms and evidence for it is gained using mutants of the model plant *Arabidopsis thaliana* or in vitro reconstituted complexes. In lycophytes the potential of PSI in photoprotection can be approached in a more straightforward way than in angiosperms, owing to the very low photosynthetic efficiency of the former, i.e., the consequence of having evolved in a CO_2-rich atmosphere. Extant lycophytes offer indeed an interesting window to look into the evolution of photoprotection in early vascular plants and may help approach experimentally some mechanisms that are (or have become) less evident in model angiosperms. A lesson learnt from *Selaginella martensii* is that photoprotective energy spillover to PSI can give rise to a non-negligible fraction of *NPQ* and, in particular, be reflected by its middle-relaxing phase, traditionally termed qT. It is improbable that the extra-qT is mechanistically separate from the ordinary qT, and neither of them is a state-transition quenching, but more likely qT is linked to energy spillover. In other words, in some plant species with a certain evolutionary history and environmental adaptation, energy spillover could be largely exploited as a background regulatory mechanism to manage light harvesting and use. In fact, correlative analyses strongly indicate that qT is primarily determined by the excitation energy pressure inside PSII and correlates with PSI core emission at 77 K and with PLhcb6. Nevertheless, although qT is already induced under low light, its relevance emerges in the carbon-limited, potentially photoinhibiting phase, when energy spillover to PSI becomes easily detectable at physiological temperature as well. PLhcb6 very probably facilitates the photoprotective use of PSI, but under the highest irradiance the full exploitation of this safe energy dissipation mechanism also requires the cooperation with phosphorylated LHCII. This result adds further complexity to the current understanding of antenna protein phosphorylation in vascular plants (reviewed in Grieco et al., 2016).

Appendix A. Fitting procedure of *NPQ* relaxation curves

The analytical method used in this work for *NPQ* relaxation study is an improvement of the method originally described by Walters and Horton (1991) with the following assumptions:

(1) each kinetic component decays exponentially;

(2) there are three decay components, called qE, qT and qI, with strongly differing characteristic decay times;

(3) qI has a decay time of hours, so it can be approximately treated as a constant;

(4) amplitudes of the decay components are additive to give rise to *NPQ* (Krause and Jahns, 2004).

A further original assumption was that all components start decaying at time 0, i.e. as soon as light is turned off (Walters and Horton, 1991). However, it was shown that this cannot be the case and the middle-relaxing component qT could start relaxing with a certain delay and this was recommended to be taken into account (Schansker et al., 2006). Relaxation curves obtained from *Selaginella martensii* include both options, so the fitting procedure was modified accordingly.

In case of no evident delay in qT relaxation, the fitting equation is a bi-exponential decay function of NPQ with respect to the time variable t:

$$NPQ = A_E\, e^{-\frac{t}{\tau_E}} + A_T\, e^{-\frac{t}{\tau_T}} + A_I \qquad \text{Eq. (A.1)}$$

where A_E, A_T, A_I are the amplitudes of qE, qT and qI components, respectively; τ_E and τ_T are the decay constants of qE and qT, respectively. The decay constant of qI is assumed to be infinite.

In case of a delay in qT relaxation, he relaxation curve is fitted with an exponential decay function in its first part, up to the delay, i.e. the quasi-plateau value of NPQ approaching time t_{delay}; the residual amplitude of $A_{T,I} = NPQ\text{-}A_E$ corresponds to the still unrelaxed qT and qI. NPQ value at t_{delay} is considered as the first point for a new exponential decay, including qT and the unrelaxable qI. Therefore, the curve is fitted as follows:

$$NPQ = \begin{cases} A_E\, e^{-\frac{t}{\tau_E}} + A_{T,I}, & 0 < t < t_{delay} \\ A_T\, e^{-\frac{t}{\tau_T}} + A_I, & t \geq t_{delay} \end{cases} \qquad \text{Eq. (A.2)}$$

It is worth noting that the fitting precision allowed by this method together with the use of a powerful curve analysis software OriginPro 2015 resulted in τ_E values smaller than those expected from the literature, *S. martensii* included (Ferroni et al., 2014; Table 1).

Appendix B. Supplementary data

Acknowledgements

This work was supported by the University of Ferrara (project FIR2016 grant assigned to L.F.) and the Academy of Finland (project 303757).

References

Akhtar P., Lingvay M., Kiss T., Deák R., Bóta A., Ughy B., Garab G., Lambrev P.H. 2016. Excitation energy transfer between Light-harvesting complex II and Photosystem I in reconstituted membranes. Biochimica et Biophysica Acta 1857, 462–472.

Aro E-M., Virgin I., Andresson B. 1993. Photoinhibition of Photosystem II. Inactivation, protein damage and turnover. Biochimica et Biophysica Acta 1143, 113-34.

Baldisserotto C., Ferroni L., Pantaleoni L., Pancaldi S. 2013. Comparison of photosynthesis recovery dynamics in floating leaves of *Trapa natans* after inhibition by manganese or molybdenum: effects on photosystem II. Plant Physiology and Biochemistry 70, 387–395.

Bellafiore S., Barneche F., Peltier G., Rochaix J.D. 2005. State transitions and light adaptation require chloroplast thylakoid protein kinase STN7. Nature 433, 892-895.

Benson S.L., Maheswaran P., Ware M.A., Hunter N., Horton P., Jansson S., Ruban A.V., Johnson M.P. 2015. An intact light harvesting complex I antenna system is required for complete state transitions in Arabidopsis. Nature Plants 1, 15176.

Bielczynski L.W., Schankser G., Croce R. 2015. Effect of light acclimation on the organization of Photosystem II super- and sub-complexes in *Arabidopsis thaliana*. Frontiers in Plant Science 7, 105.

Björkman O., Demmig-Adams B. 1995. Regulation of photosynthetic light energy capture, conversion, and dissipation in leaves of higher plants. In: Schulze ED, Caldwell MM (eds) Ecophysiology of photosynthesis. Springer, Berlin, pp 17–47.

Bos I., Bland K.M., Tianc L., Croce R., Frankel L.K., van Amerongen H., Bricker T.M., Wientjes E. 2017. Multiple LHCII antennae can transfer energy efficiently to a single Photosystem I. Biochimica et Biophysica Acta 1858, 371–378.

Bressan M., Dall'Osto L., Bargigia I., Alcocer M.J.P., Viola D., Cerullo G., D'Andrea C., Bassi R., Ballottari M. 2016. LHCII can substitute for LHCI as an antenna for photosystem I but with reduced light-harvesting capacity. Nature Plants 2, 16131.

Cazzaniga S., Dall'Osto L., Kong S.-G., Wada M., Bassi R. 2013. Interaction between avoidance of photon absorption, excess energy dissipation and zeaxanthin synthesis against photooxidative stress in Arabidopsis. Plant Journal 76, 568–579.

Croce R., Zucchelli G., Garlaschi F.M., Bassi R., Jennings R.C. (1997) Excited state equilibration in the photosystem I-light-harvesting I complex: P700 is almost isoenergetic with its antenna. Biochemistry 35, 8572–8579.

Dall'Osto L., Caffarri S., Bassi R. 2005. A mechanism of non-photochemical energy dissipation, independent from PsbS, revealed by a conformational change in the antenna protein CP26. Plant Cell, 17, 1217–1232.

Demmig-Adams B., Adams III W.W. 1996. Xanthophyll cycle and light stress in nature; uniform response to excess direct sunlight among higher plant species. Planta 198, 460-470.

Demmig B., Winter K. 1988. Characterisation of three components of non-photochemical fluorescence quenching and their response to photoinhibition. Australian Journal of Plant Physiology 163, 163–177.

Demmig B., Cleland R.E., Björkman O. 1987. Photoinhibition, 77K chlorophyll fluorescence quenching and phosphorylation of the light-harvesting chlorophyll-protein complex of photosystem II in soybean leaves. Planta 172, 378-385.

Demmig-Adams B., Cohu C.M., Muller O., Adams III W.W. 2012. Modulation of photosynthetic energy conversion efficiency in nature: from seconds to seasons. Photosynthesis Research 113, 75-88.

Demmig-Adams B., Garab G., Adams III W.W., Govindjee. 2014. Non-photochemical quenching and energy dissipation in plants, algae and cyanobacteria. Springer, New York (2014), p. 649 (ISBN 978-94-017-9031-4).

Demmig-Adams B., Muller O., Stewart J.J., Cohu C.M., Adams III W.W. 2015. Chloroplast thylakoid structure in evergreen leaves employing strong thermal energy dissipation. Journal of Photochemistry and Photobiology B: Biology 152, 357–366.

Ferroni L., Baldisserotto C., Pantaleoni L., Fasulo M.P., Fagioli P., Pancaldi S. 2009. Degreening of the unicellular alga *Euglena gracilis*: thylakoid composition, room temperature fluorescence spectra and chloroplast morphology. Plant Biology 11, 631-641.

Ferroni L., Baldisserotto C., Giovanardi M., Pantaleoni L., Morosinotto T., Pancaldi S. 2011. Revised assignment of room-temperature chlorophyll fluorescence emission bands in single living cells of *Chlamydomonas reinhardtii*. Journal of Bioenergetics and Biomembranes 43,163–173.

Ferroni L., Angeleri M., Pantaleoni L., Pagliano C., Longoni P., Marsano F., Aro E-M., Suorsa M., Baldisserotto C., Giovanardi M., Cella R., Pancaldi S. 2014. Light dependent reversible phosphorylation of the minor photosystem II antenna Lhcb6 (CP24) occurs in lycophytes. The Plant Journal 77, 893–905.

Ferroni L., Suorsa M., Aro E-M., Baldisserotto C., Pancaldi S. 2016. Light acclimation in the lycophyte *Selaginella martensii* depends on changes in the amount of photosystems and on the flexibility of the light-harvesting complex II antenna association with both photosystems. New Phytologist 211, 554–568.

Franck F., Juneau P., Popovic R. 2002. Resolution of the Photosystem I and Photosystem II contributions to chlorophyll fluorescence of intact leaves at room temperature. Biochimica et Biophysica Acta 1556, 239–246.

Gilmore A.M., Shinkarev V.P., Hazlett T.L., Govindjee. 1998. Quantitative analysis of the effects of intrathylakoid pH and xanthophyll cycle pigments on chlorophyll a fluorescence lifetime distributions and intensity in thylakoids. Biochemistry 37, 13582–13593.

Goldschmidt-Clermont M., Bassi R. 2015. Sharing light between two photosystems: mechanism of state transitions. Current Opinion in Plant Biology 25, 71–78.

Grieco M., Tikkanen M., Paakkarinen V., Kangasjärvi S., Aro E-M. 2012. Steady state phosphorylation of light-harvesting complex II proteins preserves photosystem I under fluctuating white light. Plant Physiology 160, 1896–1910.

Grieco M., Suorsa M., Jajoo A., Tikkanen M., Aro E-M. 2015. Light-harvesting II antenna trimers connect energetically the entire photosynthetic machinery – including both photosystems II and I. Biochimica et Biophysica Acta 1847, 607–619.

Grieco M., Jain A., Ebersberger I., Teige M. 2016. An evolutionary view on thylakoid protein phosphorylation uncovers novel phosphorylation hotspots with potential functional implications. Journal of Experimental Botany 67, 3883-96.

Guadagno C.R., Virzo de Santo A., D'Ambrosio N. 2010. A revised energy partitioning approach to assess the yields of non-photochemical quenching components. Biochimica et Biophysica Acta 1797, 525–530.

Hodges M., Comic G., Briantais J.-M. 1989. Chlorophyll fluorescence from spinach leaves: Resolution of non-photochemical quenching. Biochimica et Biophysica Acta 974, 289-293.

Horton P., Hague A. 1988. Studies on the induction of chlorophyll fluorescence in isolated barley protoplasts IV. Resolution of non-photochemical quenching. Biochimica et Biophysica Acta 932, 107–115.

Jahns P., Miehe B. 1996. Kinetic correlation of recovery from photoinhibition and zeaxanthin epoxidation. Planta 198, 202-210.

Jahns P., Holzwarth A.R. 2012. The role of the xanthophyll cycle and of lutein in photoprotection of photosystem II. Biochimica et Biophysica Acta 1817, 182-193.

Jajoo A, Mekala N.R., Tongra T., Tiwari A., Grieco M., Tikkanen M., Aro E-M. 2014. Low pH-induced regulation of excitation energy between the two photosystems. FEBS Letters 588, 270-274.

Järvi S., Suorsa M., Paakkarinen V., Aro, E-M. 2011. Optimized native gel systems for separation of thylakoid protein complexes: novel super and mega-complexes. Biochemical Journal 439, 207–214.

Järvi S., Suorsa M., Aro, E-M. 2015. Photosystem II repair in plant chloroplasts — Regulation, assisting proteins and shared components with photosystem II biogenesis. Biochimica et Biophysica Acta 1847, 900-909.

Joliot P.A., Finazzi, G. 2010. Proton equilibration in the chloroplast modulates multiphasic kinetics of nonphotochemical quenching of fluorescence in plants. Proceedings of the National Academy of Sciences USA 107, 12728–12733.

Itoh S., Sugiura K. 2004. Fluorescence of Photosystem I. In: Papageorgiou, G.C. and Govindjee (Eds.), Chlorophyll fluorescence: A signature of photosynthesis. Dordrecht, Kluwer Academic Publishers, pp. 231-250.

Kalaji H.M., Schansker G., Ladle R.J., Goltsev V., Bosa K., Allakhverdiev S.I., Brestic M., Bussotti F., Calatayud A., Dąbrowski P., Elsheery N.I., Ferroni L., Guidi L., Hogewoning S. W., Jajoo A., Misra A.N., Nebauer S.G., Pancaldi S., Penella C., Poli DB., Pollastrini M., Romanowska-Duda Z.B., Rutkowska B., Serôdio J., Suresh K., Szulc W., Tambussi E., Yanniccari M., Zivcak M. 2014. Frequently asked questions about in vivo chlorophyll fluorescence: practical issues. Photosynthesis Research 121, 122-158. doi: 10.1007/s11120-014-0024-6.

Kalaji H.M., Schansker G., Brestic M., Bussotti F., Calatayud A., Ferroni L., Goltsev V., Guidi L., Jajoo A., Li P., Losciale P., Mishra V.K., Misra A.N., Nebauer S.G., Pancaldi S., Penella C., Pollastrini M., Suresh K., Tambussi E., Yanniccari M., Zivcak M., Cetner M.G., Samborska I.A., Stirbet A., Olsovska K., Kunderlikova K., Shelonzek H., Rusinowski A., Baba W. 2017. Frequently asked questions about chlorophyll fluorescence, the sequel. Photosynthesis Research 132, 13-66. doi: 10.1007/s11120-016-0318-y

Kouřil R., Nosek L., Bartoš J., Boekema E.J., Ilík P. 2016. Evolutionary loss of light-harvesting proteins Lhcb6 and Lhcb3 in major land plant groups – break-up of current dogma. New Phytologist 210, 808-814.

Kovács L., Damkjær J., Kereïche S., Ilioaia C., Ruban A.V., Boekema E.J., Jansson S., Horton P. 2006. Lack of the light-harvesting complex CP24 affects the structure and function of the grana membranes of higher plant chloroplasts. Plant Cell, 18, 3106–3120.

Krause G.H., Jahns P. 2004. Non-photochemical energy dissipation determined by chlorophyll fluorescence quenching. Characterization and function. In: Papageorgiou, G.C. and Govindjee (Eds.), Chlorophyll fluorescence: A signature of photosynthesis. Dordrecht, Kluwer Academic Publishers, pp. 463-495.

Laemmli U.K. 1970. Cleavage of structural proteins during the assembly of the head of bacteriophage T4. Nature 227, 680–685.

Li X-P., Gilmore A.M., Caffarri S., Bassi R., Golan T., Kramer D., Nyiogi K.K. 2004. Regulation of photosynthetic light harvesting involves intrathylakoid lumen pH sensing by the PsbS protein. Journal of Biological Chemistry 279, 22866-22874.

Lokstein H., Härtel H., Hoffmann P., Renger, G. 1993. Comparison of chlorophyll fluorescence quenching in leaves of wild-type with a chlorophyll b-less mutant of barley (*Hordeum vulgare* L.). Journal of Photochemistry and Photobiology B, Biology 19, 217–225.

Lokstein H., Härtel H., Hoffmann P., Woitke P., Renger G. 1994. The role of light-harvesting complex II in excess excitation energy dissipation: an in vivo fluorescence study on the origin of high-energy quenching. Journal of Photochemistry and Photobiology B, Biology 26, 175–184.

Maxwell K., Johnson G.N. 2000. Chlorophyll fluorescence—a practical guide. Journal of Experimental Botany 51, 659–668.

Mekala N.R., Suorsa M., Rantala M., Aro E-M., Tikkanen M. 2015. Plants actively avoid state transitions upon changes in light intensity: role of light-harvesting complex II protein dephosphorylation in high light. Plant Physiology 168, 721–738.

Munekage Y., Hojo M., Meurer J., Endo T., Tasaka M., Shikanai T. 2002. PGR5 is involved in cyclic electron flow around photosystem I and is essential for photoprotection in Arabidopsis. Cell 110, 361-371.

Nilkens M., Kress E., Lambrev P., Miloslavina Y., Müller M., Holzwarth A.R., Jahns P. 2010. Identification of a slowly inducible zeaxanthin-dependent component of non-photochemical quenching of chlorophyll fluorescence generated under steady-state conditions in Arabidopsis. Biochimica et Biophysica Acta 1797, 466–475.

Ögren E., Rosenqvist E. 1992. On the significance of photoinhibition of photosynthesis in the field and its generality among species. Photosynthesis Research 33, 63–71

Oxborough K., Baker N.R. 1997. Resolving chlorophyll a fluorescence images of photosynthetic efficiency into photochemical and non-photochemical components—calculation of qP and F_V'/F_M' without measuring F_0'. Photosynthesis Research 54,135–142.

Pancaldi S., Baldisserotto C., Ferroni L., Bonora A., Fasulo M.P. 2002. Room temperature microspectrofluorimetry as a useful tool for studying the assembly of the PSII chlorophyll-protein complexes in single living cells of etiolated *Euglena gracilis* Klebs during the greening process. Journal of Experimental Botany 53, 1753–1763.

Pantaleoni L., Ferroni L., Baldisserotto C., Aro E-M., Pancaldi S. 2009. Photosystem II organisation in chloroplasts of *Arum italicum* leaf depends on tissue location. Planta 230, 1019–1031.

Passarini F., Wientjes E., Hienerwadel R., Croce R. 2009. Molecular basis of light harvesting and photoprotection in CP24. Journal of Biological Chemistry 284, 29536–29546.

Peek M.S., Russek-Cohen E., Wait D.A., Forseth I.N. 2002. Physiological response curve analysis using nonlinear mixed models. Oecologia 132, 175–180.

Porra R.J., Thompson W.A., Kriedemann P.E. 1989. Determination of accurate extinction coefficients and simultaneous equations for assaying chlorophyll a and chlorophyll b extracted with 4 different solvents – verification of the concentration of chlorophyll standards by atomic-absorption spectroscopy. Biochimica et Biophysica Acta 975, 384–394.

Pribil M., Pesaresi P., Hertle A., Barbato R., Leister D. 2010. Role of plastid protein phosphatase TAP38 in LHCII dephosphorylation and thylakoid electron flow. PLoS Biology 8, e1000288.

Pursiheimo S., Rintamäki E., Baena-Gonzalez E., Aro E-M. 1998. Thylakoid protein phosphorylation in evolutionally divergent species with oxygenic photosynthesis. FEBS Letters 423, 178–182.

Quick W.P., Stitt M. 1989. An examination of factors contributing to non-photochemical quenching of chlorophyll fluorescence in barley leaves. Biochimica et Biophysica Acta 977, 287-296.

Rantala M., Lehtimäki N., Aro E-M., Suorsa M. 2016. Downregulation of TAP38/PPH1 enables LHCII hyperphosphorylation in Arabidopsis mutant lacking LHCII docking site in PSI. FEBS Letters 590, 787–794.

Rantala M., Tikkanen M., Aro E-M. 2017. Proteomic characterization of hierarchical megacomplex formation in *Arabidopsis* thylakoid membrane. The Plant Journal, doi 10.1111/tpj.13732.

Rintamäki, E., Martinsuo, P., Pursiheimo, S. and Aro, E-M. 2000. Cooperative regulation of light-harvesting complex II phosphorylation via plastoquinol and ferredoxin-thioredoxin system in chloroplast. Proceedings of the National Academy of Sciences USA 97, 11644–11649.

Rochaix J-D. 2013. Redox regulation of thylakoid protein kinases and photosynthetic gene expression. Antioxidants and redox signaling 18, 2184-2201.

Schansker, G., Toth S.Z., Strasser, R. (2006) Dark recovery of the Chl a fluorescence transient (OJIP) after light adaptation: the qT component of the non-photochemical quenching is related to an activated photosystem I acceptor side. Biochimica et Biophysica Acta 1757, 787–797.

Shapiguzov A., Ingelsson B., Samol I., Andres C., Kessler F., Rochaix J.D., Vener A.V., Goldschmidt-Clermont M. The PPH1 phosphatase is specifically involved in LHCII dephosphorylation and state transitions in Arabidopsis. Proceedings of the National Academy of Sciences USA 107, 4782-4787.

Schlodder E., Cetin M., Byrdin M., Terekhova I.V., Karapetyan N.V. 2005. $P700^{+}$- and $^{3}P700$-induced quenching of the fluorescence at 760 nm in trimeric Photosystem I complexes from the cyanobacterium *Arthrospira platensis*. Biochimica et Biophysica Acta 1706, 53-67.

Schumann T., Paul S., Melzer M., Dörmann P., Jahns P. 2017. Plant growth under natural light conditions provides highly flexible short-term acclimation properties toward high light stress. Frontiers in Plant Science 8, 681.

Sonoike K. 2011. Photoinhibition of Photosystem I. Physiologia Plantarum 142, 56-64.

Suorsa M., Järvi S., Grieco M., Nurmi M., Pietrzykowska M., Rantala M., Kangasjärvi S., Paakkarinen V., Tikkanen M., Jansson S., Aro E-M. 2012. PROTON GRADIENT REGULATION5 is essential for proper acclimation of Arabidopsis photosystem Ito naturally and artificially fluctuating light conditions. Plant Cell 24, 2934–2948.

Suorsa M., Rantala M., Mamedov F., Lespinasse M., Trotta A., Grieco M., Vuorio E., Tikkanen M., Järvi S., Aro E-M. 2015. Light acclimation involves dynamic re-organisation of the pigment-protein megacomplexes in non-appressed thylakoid domains. The Plant Journal 84, 360–373.

Tikhonov A.N. 2015. Induction events and short-term regulation of electron transport in chloroplasts: an overview. Photosynthesis Research 125, 65–94.

Tikkanen M., Aro, E-M. 2014 Integrative regulatory network of plant thylakoid energy transduction. Trends Plant Sci. 19, 10–17.

Tikkanen M., Piippo M., Suorsa M., Sirpiö S., Mulo P., Vainonen J., Vener A.V., Allahverdiyeva Y., Aro E-M. 2006. State transitions revised – a buffering system for dynamic low light acclimation of Arabidopsis. Plant Molecular Biology 62, 779–793.

Tikkanen M., Nurmi M., Suorsa M., Danielsson R., Mamedov F., Styring S., Aro E-M. 2008. Phosphorylation-dependent regulation of excitation energy distribution between the two photosystems in higher plants. Biochimica et Biophysica Acta 1777, 425–432.

Tikkanen M., Grieco M., Kangasjärvi S., Aro E-M. 2010. Thylakoid protein phosphorylation in higher plant chloroplasts optimizes electron transfer under fluctuating light. Plant Physiology 152, 723–735.

Tiwari A., Mamedov F., Grieco M., Suorsa M., Jajoo A., Styring S., Tikkanen M., Aro E-M. 2016. Photodamage of iron-sulphur clusters in photosystem I induces non-photochemical energy dissipation. Nature Plants 2, 16035.

van Kooten O., Snel J.F.H. 1990. The use of chlorophyll fluorescence nomenclature in plant stress physiology. Photosynthesis Research 25, 147-150.

van der Weij-de Wit C.D., Ihalainen J.A., van Grondelle R., Dekker J.P. 2007. Excitation energy transfer in native and unstacked thylakoid membranes studied by low temperature and ultrafast fluorescence spectroscopy. Photosynthesis Research 93, 173–182.

Verhoeven A.S., Adams III W.W., Demmig-Adams B. 1996. Close relationship between the state of the xanthophyll cycle pigments and photosystem II efficiency during recovery from winter stress. Physiologia Plantarum 96, 567-576.

Walters R.G., Horton P. 1991. Resolution of components of non-photochemical chlorophyll fluorescence quenching in barley leaves. Photosynthesis Research 27, 121–133.

Walters R.G., Horton P. 1993. Theoretical assessment of alternative mechanisms for non-photochemical quenching of PS II fluorescence in barley leaves. Photosynthesis Research 36, 119–139.

Wientjes E., van Amerongen H., Croce R. 2013a. LHCII is an antenna of both photosystems after long-term acclimation. Biochimica et Biophysica Acta 1827, 420–426.

Wientjes E., Drop B., Kouřil R., Boekema E.J., Croce R. 2013b. During state 1 to state 2 transition in *Arabidopsis thaliana*, the photosystem II supercomplex gets phosphorylated but does not disassemble. Journal of Biological Chemistry 288, 32821-32826.

Yokono M., Takabayashi A., Akimoto S., Tanaka A. 2015. A megacomplex composed of both photosystem reaction centres in higher plants. Nature Communications 6, 6675.

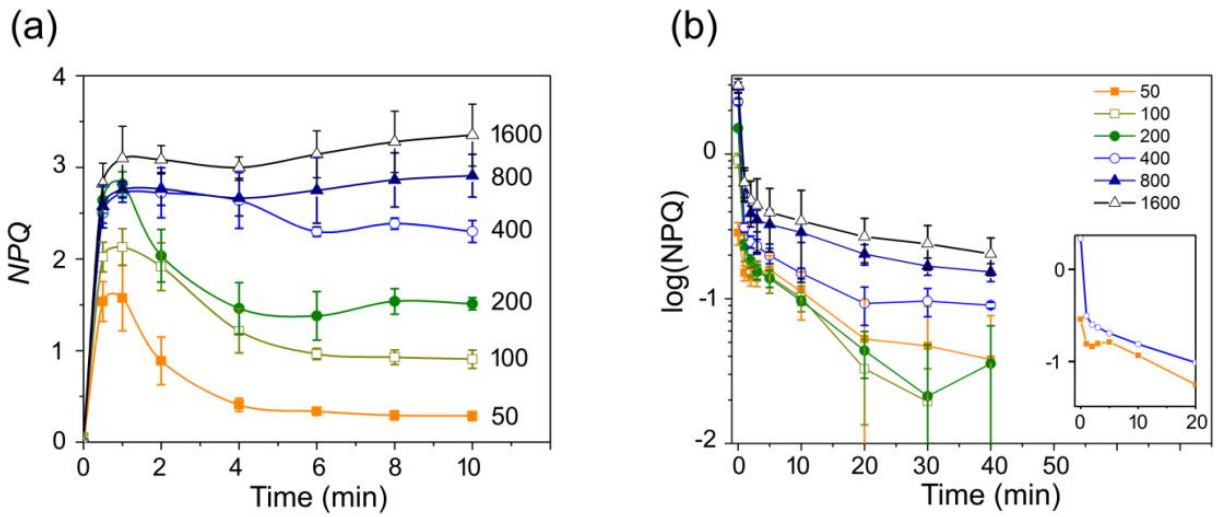

Fig. 1. Induction and dark relaxation of *NPQ* in *Selaginella martensii*. (a) NPQ induction kinetics during 10 min exposure to actinic light of different intensity, as indicated in the graph. (b) NPQ relaxation kinetics in darkness after exposure to actinic light as in (a). NPQ values are reported in logarithmic scale to allow linearization of exponentially decaying components. In the insert, two examples of relaxation kinetics behavior show the presence or absence of a delay in qT component relaxation. Values are means of n = 3 ± SD.

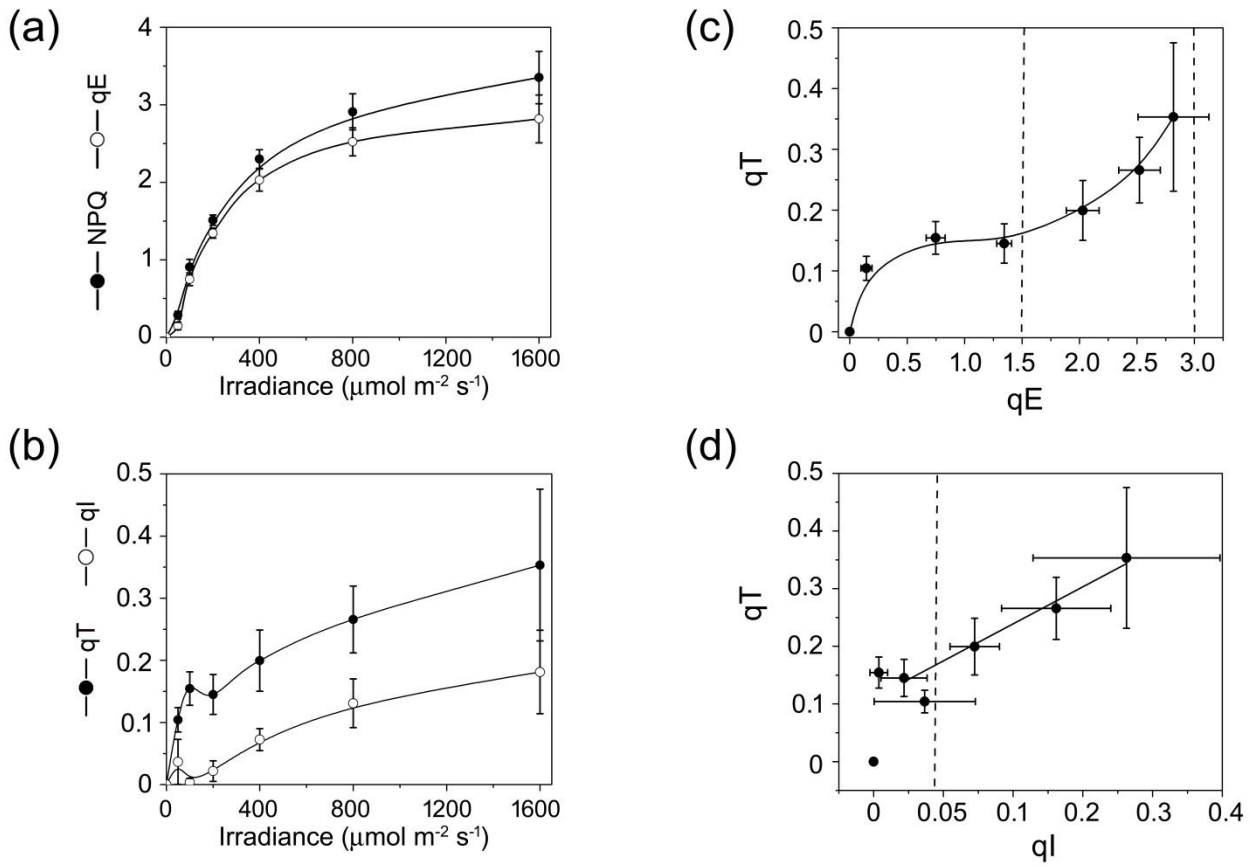

Fig. 2. Light curves of *NPQ* and its kinetic components in *Selaginella martensii* after a 10 min exposure to actinic light. (a) Light curves of NPQ and its main component, the fast decaying "energy quenching" qE. (b) Light curves of the middle phase in NPQ relaxation, indicated as qT, and the slowest photoinhibitory component qI. (c) qT *versus* qE relationship. The two dotted lines approximate the qE value corresponding to the induction of the extra-qT and the qE saturation value. (d) qT *versus* qI relationship. The dotted line approximates the onset of photoinhibition; a linear regression was calculated using the last four points (see panel b of this Figure). Values are means of N = 3 ± SD.

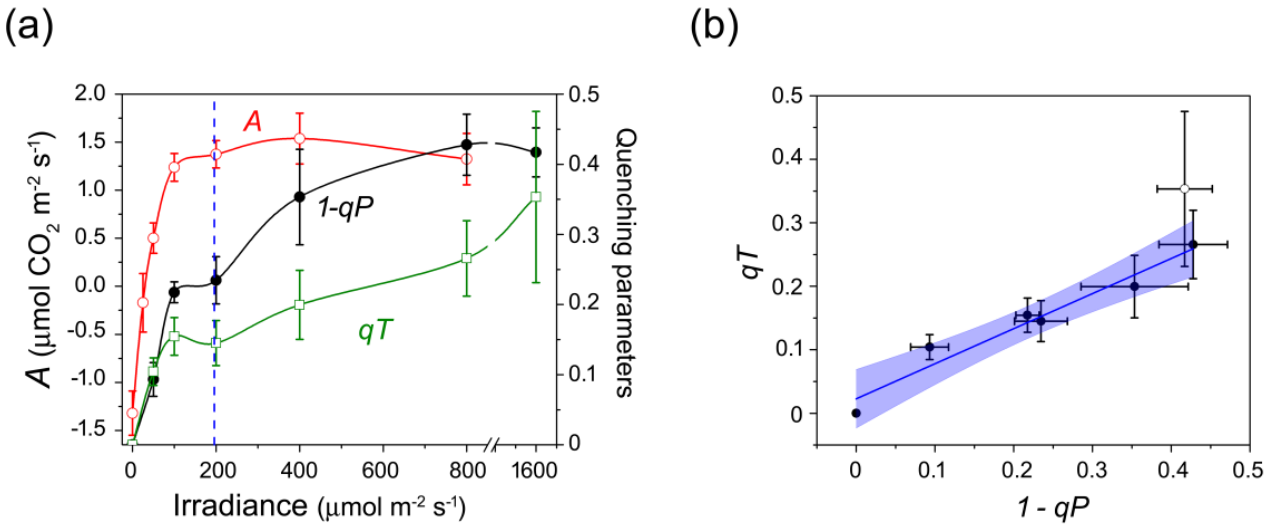

Fig. 3. Relationship between qT and photosynthetic capacity in *Selaginella martensii*. (a) Comparative representation of light curves of excitation energy pressure inside PSII (1-qP), steady-state net photosynthesis (*A*) and qT. The dotted line indicates the irradiance giving rise to saturation of the carbon fixing capacity, in particular 95% A_{max}. Values are means of N = 3 ± SD for the fluorescence quenching parameters, N = 4 ± SE for the gas exchange. (b) qT *versus* 1-qP correlation. The regression line is indicated with 95% confidence bands. The outlier point corresponding to 1600 mmol m^{-2} s^{-1} was excluded from the regression calculation and is shown with an open circle symbol.

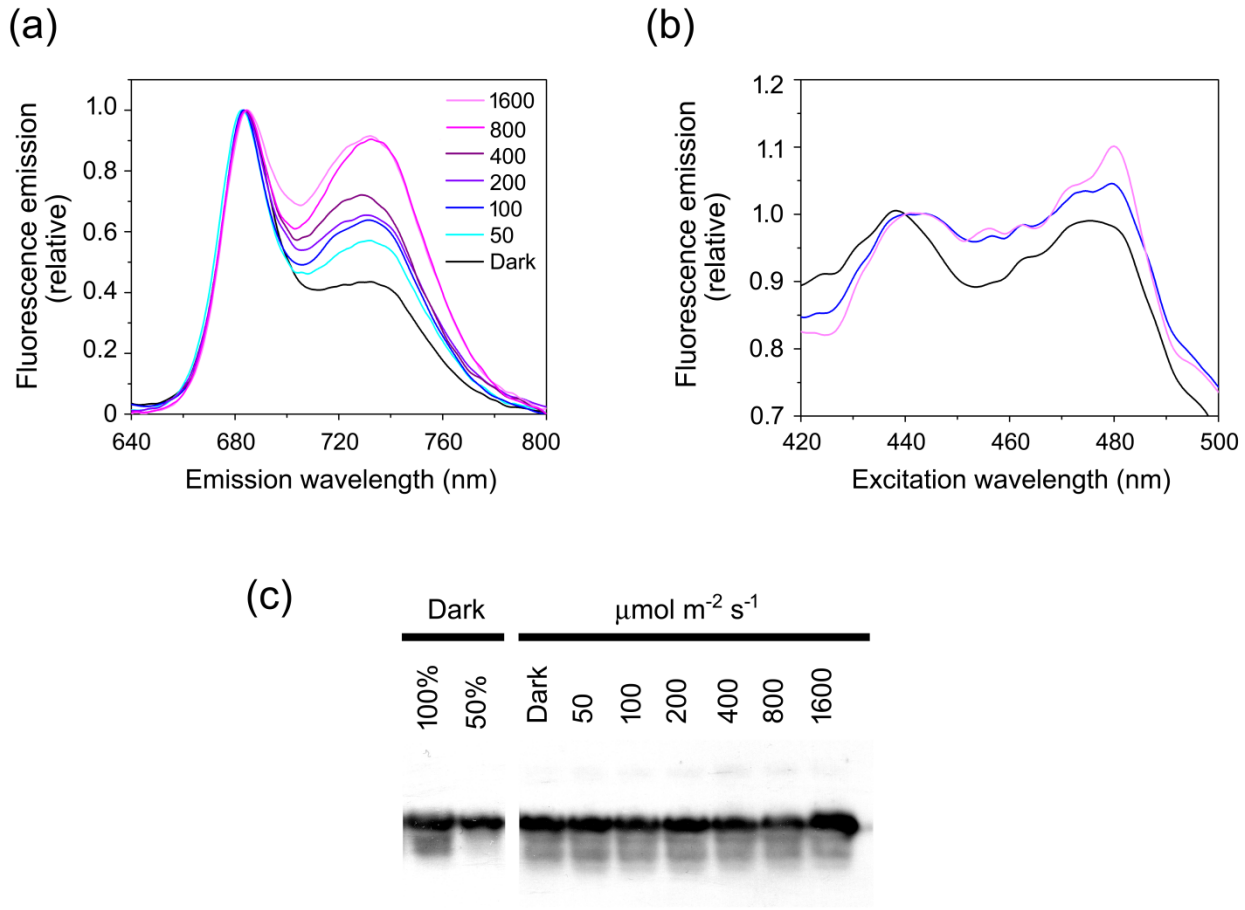

Fig. 4. Low-temperature in vivo fluorescence spectroscopy of *Selaginella martensii* leaves. (a) Fluorescence emission spectra recorded at 77 K from leaves exposed to different light intensities, as indicated. Excitation wavelength was at 436 nm and spectra were normalized to PSII emission at ca. 685 nm. (b) Fluorescence excitation spectra recorded at 77 K from leaves after dark-acclimation or after exposure to 100 or 1600 µmol m^{-2} s^{-1}, color legend as in (a). Emission from PSI was detected at 730 nm and normalized to the Chl *a* band at 440 nm, which was set to 1. Chl *b* is responsible for the peak at ca. 480 nm. (c) Immunodetection of D1 protein of PSII reaction center reveals no relevant depletion of D1 content in thylakoids isolated from leaves exposed to irradiance up to 1600 µmol m^{-2} s^{-1} for 1 h. Lanes were loaded with 1 µg Chl. On the left, a loading control with 1 and 0.5 µg Chl from dark-acclimated sample.

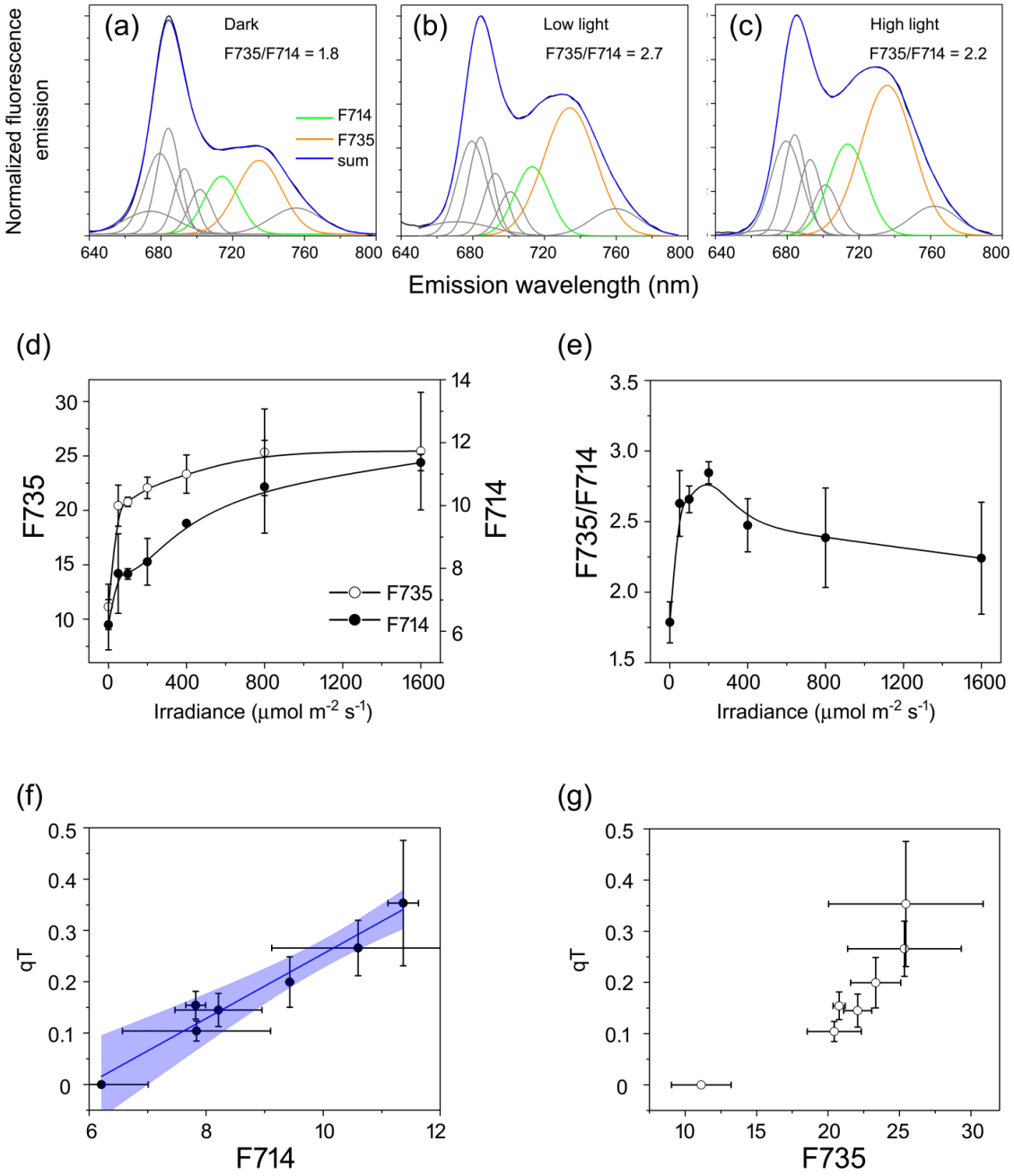

Fig. 5. Relationship between PSI fluorescence emission bands at low temperature and qT in Selaginella martensii. (a-c) Representative Gaussian deconvoluted 77 K emission spectra of leaves acclimated to darkness (a), low light (b, 100 µmol m^{-2} s^{-1}), high light (c, 1600 µmol m^{-2} s^{-1}). Fluorescence spectra were normalized to PSII peak at 685 nm before deconvolution. Emission from PSI and LHCI was resolved as the two components F714 and F735. (d) Light-dependence of F714 and F735. Band intensity corresponds to the area subtended under the corresponding Gaussian components. Note that the y axes were set differently for F714 and F735 to allow an easier comparison. (e) F735/F714 fluorescence emission ratio. (f)) qT *versus* F714 correlation. The regression line is indicated with 95% confidence bands. (g) qT *versus* F735 data plot. All fluorescence data points are means of *N*=3 with SD.

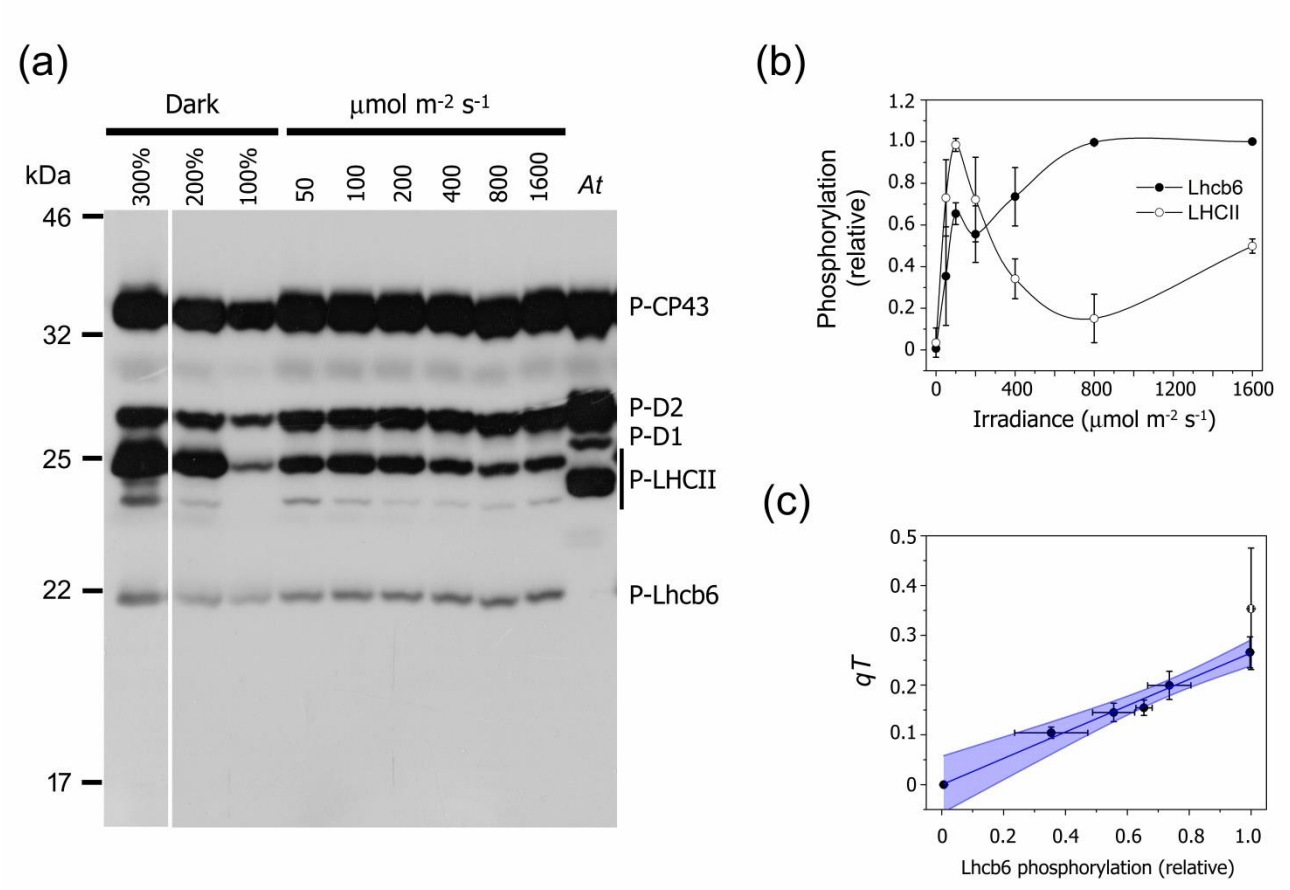

Fig. 6. Steady-state thylakoid protein phosphorylation in *Selaginella martensii*. (a) Immunodetection of thylakoid phosphoproteins using an anti-phosphothreonine antibody (core antenna complex of photosystem II, C43; D1 and D2 proteins of photosystem II reaction centre; major light-harvesting complex II proteins, LHCII; CP24 antenna protein of photosystem II, Lhcb6). Phosphoproteins were analyzed in *S. martensii* after different light treatments and in *Arabidopsis thaliana* (At) under growth light. Lanes were loaded with 1 µg Chl. (b) Relative band intensity of phosphorylated LHCII and Lhcb6. Band volumes were double normalized and means of N = 2-4 ± SD are shown. Double normalization procedure is explained in Supplementary Fig. S1. (c) Lhcb6 phosphorylation level *versus* qT correlation. The regression line is indicated with 95% confidence bands. The outlier point corresponding to 1600 mmol m^{-2} s^{-1} was excluded from the regression calculation and is shown with an open circle symbol.

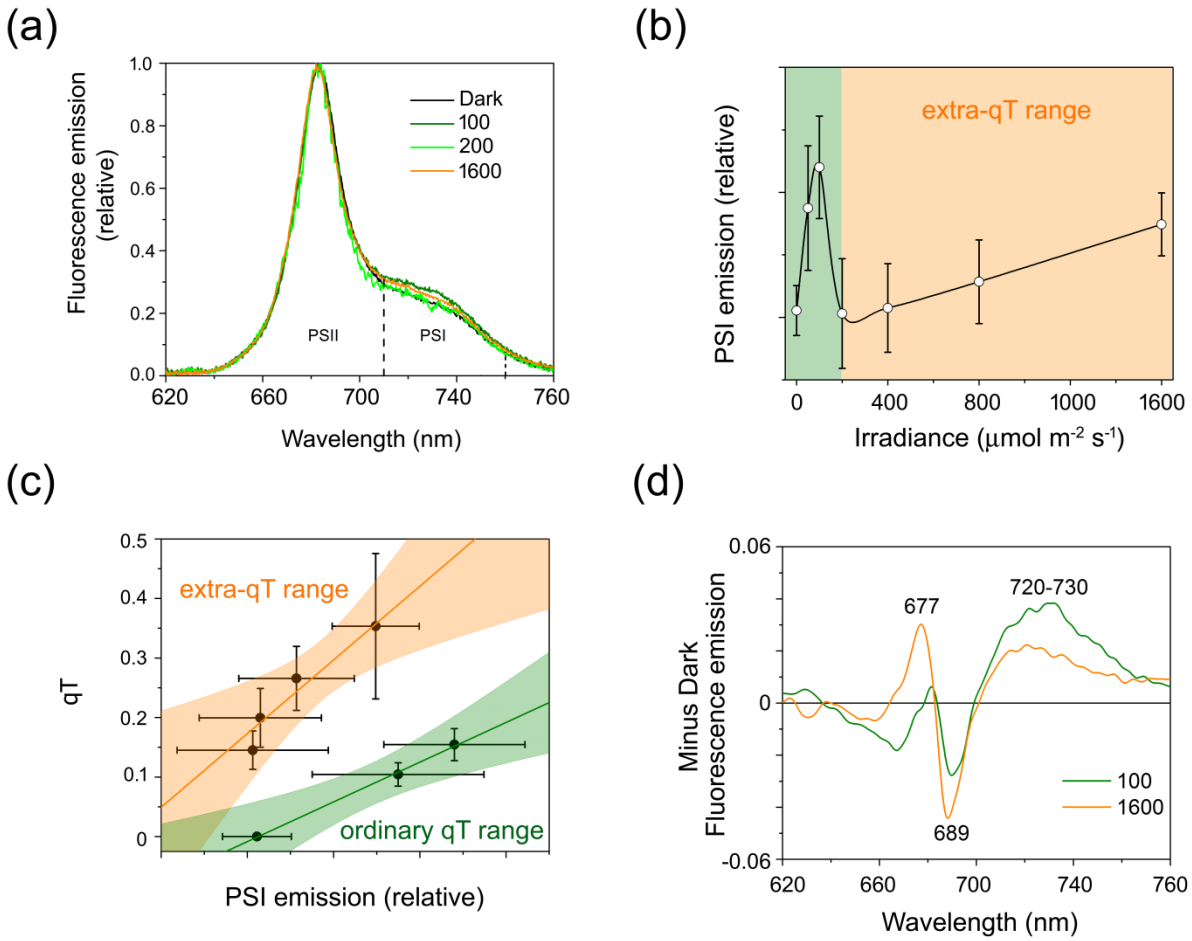

Fig. 7. Steady-state room-temperature fluorescence emission spectra of *Selaginella martensii*. (a) Normalized fluorescence emission spectra in the dark-acclimated state or after exposure to actinic light with different intensity; vertical dotted lines approximate the emission region dominated by PSII or PSI. Original spectra were corrected for baseline and normalized to their maximum. (b) Realtive PSI emission intensity. For each irradiance treatment, PSI emission was obtained as the area subtended under the double normalized spectra between 710 and 750 nm; the green background approximates the range of the ordinary qT, while the orange background that of the extra-qT. Values are means of N = 6-14 ± SE. (c) qT *versus* PSI emission correlation. Two regression lines are drawn with 95% confidence bands. (d) Difference spectra between light-treated and dark-acclimated terminal branches.